

Cumulative response to Referee#1 and #2

tc-2021-73

August 13, 2021

We thank both referees for their valuable comments and suggestions that significantly improve the quality of the manuscript. In this cumulative response we first reply to Referee#1 and then to Referee#2. To avoid redundancy, we refer to responses to the other referee whenever appropriate. Note, that we refer to three different versions of the manuscript in our replies: 1) the original version of the manuscript (equivalent to production file) to which the referees responded and to which all mentioned line numbers refer, 2) the revised manuscript already including many of the referee's suggestions that can be retraced in the attached latexdiff file generated with the original version, and 3) the final version of the manuscript, for which we propose changes, but that have not yet been implemented. It will rather be submitted and prepared after the editor's decision.

Colour code:

Black: Referee comments

purple: Author responses

1 Referee#1 comments

This paper describes a modular Eulerian-Lagrangian approach solving the coupled non-linear processes. The authors report the shortcomings of the majority of snow models that do not give an explicit numerical solution of the ice mass continuity equation but are built around. The model formulation of the snow scheme presented explicitly accounts for the ice mass balance and couples mechanical settling, heat transport and vapour transport whereby these processes can also be analysed individually due to the modular structure of the model. This modular design of the new approach allows for high degree of flexibility, which the authors use to analyse different isolated and coupled scenarios involving of heat transport, vapour transport and mechanical settling of a dry two-layer snowpack. The work provides a good basis for future work and discussions on the future generation of snow models. The work is very exciting and gives new approaches that will be useful for the snow modelling community. However, I have some suggestions for changes in restructuring of the work and some visualisations.

1.1 Major Comments:

1. The discussion section lacks comparisons to other studies and observations from which one can see the progress. This would provide an important context for the presented results and an evaluation of the presented results of the different cases and model behaviour. More discussion and comparison would for example be desirable in section 4.2: are there other studies that show the same? Also section 4.3: How about a comparison to observations and other work

e.g. for lines 408 to 410?

We agree to the referee that a comparison of the implemented process model with data from lab experiments or field observations would be very valuable to the community and is a necessary next step in going forward. After intense discussion, we have decided to stick to the original scope of the manuscript, namely to discuss synthetic examples only. We still believe that our paper is of value-add to the research community due to the following reasons:

- A number of papers exist that compare process models with observations. Only few papers, however, compare the different process building blocks and corresponding explicit statement of their generic and numerical approaches. We deliberately focus on the synthetic model as it allows us to conduct a systematic qualitative and quantitative investigation of the coupling between the individual process building blocks. Including a comparison to data at the same level of detail would imply a significant extension to the existing manuscript.
- Our aim with this manuscript is to report on analytical findings to prepare the development of a new rigorous, generic snowpack model. Specifically, we see our progress as an extension of Hansen and Foslien (2015)'s model, namely the consideration of settling, which is one of the novelties in our work.
- While our computational model facilitates the above analysis, its current development stage does not allow for a meaningful comparison to experimental, or field data. This would require significant extensions to the code and the text, and is beyond the scope of this paper also in light of the 12 pages specification of TC that are already exceeded.
- In order to connect our synthetic results better with relevant physical regimes, we propose to a) elaborate at a greater level of detail on the model parameters used in this manuscript, for instance deposition rates or settling velocities, as this will help the reader to categorize simulated magnitudes, and b) we suggest to include an additional (yet also synthetic) numerical test case based on the suggestion of Referee#2 (line 420) with thin snow layers at the top and bottom of the snowpack. This test case points towards the feasibility of potential future comparative studies with detailed and more complex snowpack data.

2. The authors also use references sparingly in the method sections. For example, section 2.3 get along without using a single reference. If this is a result of the author's work, I recommend emphasising this to the reader.

Thanks for the remark. We assume that you refer to Sect. 2.2. because Sect. 2.3 has a number of references. We provide an extensive state of the art, and therefore decided to keep the text in the method's section slim. However, we agree that it is important to point out the sources that inspired our method's section. In the revised manuscript, we therefore included several references into the method's section as well.

3. I recommend restructuring section 4 and using a separate method section for the difference steps you took to apply the model. I suggest moving line 363 – line 379 to a subsection of the methods. I also recommend moving section 4.1 to the methods. For me, the results section starts with line 392.

Thanks for the suggestion. We included that in the revised manuscript and moved line 363 - line 379 to Section 3.6 **Application of the model** and Section 4.1. to Section 3.7 and made some small adjustments resulting from the structure changes in the text.

4. Section 4.6 and Fig. 10: Here you write that you compare cases 5 and 8 and use Fig. 10 for visualisation. However, Fig. 10 only visualise for case 8. I can only find the visualisation for

case 5 in Fig. 6 and 7 but only for different variables or different visualisation. This makes it difficult for the reader to compare the two cases. I suggest adding the visualisation for case 5 in Fig. 10. Also, I cannot find a comparison to case 5 in the text. You describe Fig. 10, briefly compare your results to section 4.2, which deals with case 1, and mention the sublimation peak as observed for other cases. However, I cannot find a comparison to case 8.

This is a good comment. Indeed no comparison to linear Glen’s law was included in the original version of the manuscript so that the original subsection title was misleading. In the revised manuscript, we changed the subsection title to **Non-linear Glen’s law in a fully coupled dry snowpack model of constant viscosity (Case 8)**. We decided to keep a brief comparative discussion of the settling profiles corresponding to linear versus non-linear Glen’s law in the text of the revised manuscript. In doing so, we refer to the linear version of the settling profile for Case 1 in the previous Fig. 4 for comparison with Case 8. Although Case 1 in Fig. 4 is not fully coupled (in contrast to Case 8) the velocity profile can be used for meaningful comparison between the two.

1.2 Detailed Comments:

- **Line 20:** I suggest to add “e.g. Snowpack, Crocus” behind “when not even detailed snowpack models”.
Done!
- **Line 29:** Please name the snowpack models.
We named the snowpack models and added SNOWPACK and Crocus in the revised manuscript.
- **Line 46:** The vapour transport is very important and interesting. I encourage the authors to explore further the importance and the differences in e.g. alpine and arctic snow of the importance.
Thanks for the remark. In the revised manuscript, we elaborated further on the differences of vapor transport in alpine and arctic snow as follows:
Temperature gradients between ground and atmosphere imply upward vapor fluxes in snowpacks. Stronger temperature gradients (either due to a smaller snowpack height or colder surface temperature) in the Arctic yield higher vapor fluxes (Domine et al. 2019) compared with alpine snowpacks. Depth hoar layer with reduced density and thermal conductivity form at the snowpack’s bottom. In alpine snowpacks similar hoar layers develop within the snowpack that may cause avalanches due to their low mechanical stability (Schweizer et al. 2003).
- **Line 50-52:** See comment above: Please describe in more detail why it is important.
This is answered in the previous comment for line 46.
- **Line 57:** Please also add the details for Crocus.
We agree with this comment. However, we could not find a discussion on explicit time step constrains in the literature. We found possible time step sizes of 15 min in Viallon-Galinier et al. (2020); Brun et al. (1989) and 1 hour in combination with other models in Vionnet et al. (2012) and added these details to the revised manuscript.
- **Line 61:** You mention that a finer spatial resolution is needed. Please mention the spatial resolution of SNOWPACK and Crocus. We agree with the referee that this information would be valuable. We added the possible values for layer thicknesses based on a literature study to the revised manuscript. We found that the minimum layer thickness in Crocus is 0.5 cm (Brun et al. 1989). An upper limit for layer thickness is not stated in the referenced literature. In

SNOWPACK, a typical layer thickness is 2 cm (Wever et al. 2016) but can also reduce to 0.01 cm (Jafari et al. 2020). Explicit ranges that constrain layer thicknesses in SNOWPACK and Crocus are not given in the referenced literature.

- **Line 74:** Reference is needed for the current treatment of densification in snowpack models. We added references to the revised manuscript.
- **Line 80:** Define “ σ -coordinates”. σ -coordinates are used in a number of disciplines, yet are particularly well known from oceanography: The ocean’s surface and bottom are projected on coordinates $\sigma = 0$ and $\sigma = -1$ that follow the ocean floor’s topography. We included a definition in the revised manuscript.
- **Line 111:** Please add a reference where this common starting point is used in snow models. We added references and an explanation to the revised manuscript.
- **Line 113:** I recommend deleting “without explicitly mentioning every time”. You already write “if not stated otherwise”. We followed the referee’s suggestion and deleted it in the revised manuscript.
- **Line 115:** “snow density” did you mean “ice density” ? Please clarify. Thanks for the remark. We meant snow density. We reformulated this passage in the revised manuscript for clarification.
- **Line 114-117:** Reference is needed here. We added references to the revised manuscript.
- **Line 119:** Would there be a lot change if wet snow were used? Please clarify in 2-3 sentences the differences that dry snow and wet snow would make (more detailed description of what you have already started in line 121). Thanks for the remark. In the original manuscript, we discuss how to incorporate water in the summary and conclusions section. In response to your comment, we referenced in line 122 the summary and conclusions section for details, and we extended the corresponding discussion in the revised manuscript.
- **Line 121:** I recommend adding “compared to wet snow situation” after “as the more challenging (yet less investigated) one” We added the referee’s suggestion.
- **Line 122:** I suggest starting a new paragraph for “Note, that water transport ...” We adjusted the paragraph.
- **Table 1:** Is there a value missing for density? I suggest ordering the variables within the headings according to their occurrence in the equations. So ice volume fraction first, followed by vertical velocity, etc. This is a helpful suggestion. We changed the table accordingly in the revised manuscript. Air density is now included. Furthermore, we noticed that k_i and k_a are not used in the paper and deleted them, while stress related parameters are not listed yet and included them. We changed the name "Effective model parameters of snow" to "Model parameters of snow". We changed the term ρ_{eff} to ρ_{snow} (consistently in the whole manuscript).
- **Line 129:** “source term c” do you mean ice deposition rate? Thanks for the remark! Indeed, this can be understood as the ice deposition rate. However,

our intention is to keep c more general since it can also refer to more processes such as ice production/loss by freezing/melting additional to sublimation/deposition. We therefore decided to keep the general definition of c in the beginning of the methods sections, also due to the comment on line 132-134 that asks for the impact of melting on the continuity response. We also added an additional clarifying explanation in the revised manuscript.

- **Line 132 – 134:** You write that vertical motion results either from mechanical settling changes in ice volume from sublimation/deposition. What about melting and snow redistribution?
We added melting and freezing as contributors to the source term and the continuity response in the revised manuscript. Snow redistribution in form of compaction, heat and vapor transport as well as phase changes is included in the vertical motion.
- **Line 139:**
see comment for line 129
See our reply to comments for line 129 and line 132-134.
- **Line 141:** “Hence we will refer to c as the deposition rate” I suggest to introduce this term earlier maybe line 129 (see comments line 129, line 139)
See our reply to comments for line 129 and line 132-134.
- **Line 152:** Please add references for snowpacks where the approach typically chosen in the snowpack models is apparent.
This is a good comment. Thanks for that! Even though this stress-strain relation is not explicitly stated in the literature of detailed snowpack models, these models implicitly fall back on this standardized approach. We added references, and for clarification we replaced ‘typically’ by ‘implicitly’ in the revised manuscript.
- **Line 170:** Which properties of the snow microstructure? We added the properties to the revised manuscript.
- **Line 185f:** Define g (only defined in line 299).
We included the definition for g and also deleted ‘Here,’ in the revised manuscript.
- **Line 186:** Please define the term “snowpack’s effective density” Thanks for the remark. We rather call it snow density, which is more intuitive, and changed it at all locations including Table 1 in the revised manuscript.
- **Line 189:** Please define ζ .
We defined ζ as the integration variable in the revised manuscript.
- **Line 203 – 210:** First, you write that you are extending the model for mechanics but a few lines later you write “and thus it is neglected in the following.” I cannot follow this thought. Please clarify This is a valuable comment, thanks! We agree that this was not clear in the original version of the manuscript. Our approach is as follows: We extended the model by Hansen and Foslien (2015) for mechanics. The convective term in the vapor equation arises from the mechanics. However, its impact on deposition rate, temperature, etc. is very low compared to that of diffusion. Thus, we neglect it in the remainder and essentially use the model by Hansen and Foslien (2015). To avoid any confusion, we deleted the sentences that discuss the mechanics extension and deleted the convective term from the vapor mass balance in the revised manuscript. This does not affect any of our results and conclusions!

- **Line 214 – 215:** “Instead of following [...] closure for the source term” repetition of line 202. I suggest to add the references mentioned in line 215 to line 202 and delete 214-215.
Nice suggestion! We included this comment in the revised manuscript.
- **Line 244:** What do you mean with “necessary accuracy”? Please add a sentence what the necessary accuracy for the scenarios is.
Thanks for the remark! We agree that ‘necessary accuracy’ does not make sense in this context. We replaced ‘results at the necessary accuracy’ by ‘is applicable to the’ in the revised manuscript.
- **Line 245:** I suggest to add “using a 1d snow column” at the end of the sentence “[...] scenarios considered in the paper.” We incorporated this comment in the revised manuscript.
- **Line 247:** “In that situation”. Which situation do you mean with “that”? What is a complex geometry in this context? 2d/3d? Thanks for the remark. What we mean with ‘that situation’ is a finite element solution. With complex geometry, we mean snowpacks that, for instance lay on a mountain slope. We reformulated the sentence in the revised manuscript to make that clearer.
- **Line 252:** For the interested reader, it would be helpful to add an example reference for the use of a second order Strang splitting. We added a reference to [LeVeque \(2002\)](#) to the revised manuscript, in which the splitting is described.
- **Line 275:** You only explain the usage of a Lagrangian approach in this line but already use the term before in line 237. I recommend moving this explanation to an earlier line.
Thanks for the comment! We added an explanation to **Step 1** in the same style as for **Step 2** in the revised manuscript. We did not change the content of line 275, as we believe it increases readability.
- **Line 301:** What about Crocus? Please add reference here. We agree that it would be nice to include this information regarding Crocus. Yet, it is neither stated explicitly in the Crocus references nor did we find it after screening the source code.
- **Line 313:** “within”
Corrected!
- **Line 323:** Define α .
 α fulfills the role of a generalized density times heat capacity (ρc_p). It is used to formulate a generic numerical scheme, which is the aim of our work. Note, that we added the right hand side of the generalized equation (Eq. 21), which was missing in the original manuscript.
- **Figure 2:** Nice and helpful overview. I suggest inserting the names of Calonme, and Hansen and Folien in the boxes of the approaches and the equation numbers used to give the reader a quick overview.
This is a good suggestion. We will change the figure accordingly in the final version of the manuscript.
- **Line 347:** Figure appears in manuscript before it is mentioned in the paper.
We will pay attention to that when preparing the final version of the manuscript.
- **Line 349:** What is the minimum time step for the output? Does it also vary?
Thank you for this comment. In our approach, we chose a dynamic time step adaptation

based on the mesh Fourier number. In response to settling processes, the mesh sizes in our test cases vary and decrease, and so does the time step. At initiation the time step is in the range of 1 min. After 2 days simulation time the time step decreases to a few seconds and after 4 days simulation time to thirds of seconds. In our test cases, the time step size is mostly dominated by the mesh size. In order to facilitate longer simulations runs, one could think of merging homogeneous neighboring cells either after regular time instants, e.g. after a specific time period (day), or whenever a certain time step threshold is undercut. However, this is future work, and we did not explore it in the current study. We added some sentences on the decreasing time step size, and we corrected the equation by adding the subscript k to the formula in the revised manuscript. We will include a short discussion on the time step evolution in the summary and conclusions section of the final manuscript.

- **Line 351 – 356:** Already in Figure 2. Please bring both information together in Figure 2 (see also comment about Figure 2).
We agree to this comment and reorganized text and caption in the revised manuscript. Additionally, we moved the last three sentences of the caption of Fig. 2 to the text (following Referee#2's comment on Figure 2).
- **Line 360:** I recommend deleting “(Sect. 4)”
We deleted (Sect. 4) in the revised manuscript.
- **Line 383:** “The densities are in the range of [...]” For which regions/ type of snow is this the case?
Thanks for the remark. Here, we are not inspired by snow in a particular geographic region, but wanted to present an extreme and very active snow regime. The layered snowpack with small snow densities ensure strong dynamical coupling of the processes. We will include a discussion of geographical locations, where these snow densities/snowpacks can be found in the final version of the manuscript.
- **Line 384:** Correct “over over”.
Corrected!.
- **Figure 3:** Why do you choose these densities? Why does your layer have equal thickness? Representative for what region? Why do you use the values for ice volume, representative for what? Any reference for the used values?
See the response to your previous comment on line 383.
- **Line 392:** I recommend changing “As the first step” to “first”
We changed it in the revised manuscript.
- **Line 394:** “Furthermore, the vertical velocity varies less in the upper layer than it does in the lower layer.” Misleading formulation, difficult to understand on first reading. Please clarify: in comparison of the same time step or between/within time steps?
Thank you for this comment. We meant within one time step. We reformulated the sentence in the revised manuscript.
- **Line 397:** Does it increase at all in the upper layer? I can only see the thinning of the snowpack but no colour changes in the upper layer.
Ice volume fraction also increases in the upper layer. However, the increase is small and not easily seen. We will adjust the color bar levels to improve visibility in the final version of the paper.

- **Line 398:** “the extent of the upper layer decreased only slightly with time”, how many cm at the end?
It decreases by approximately 3.5 cm. We included this information in the revised manuscript.
- **Figure 4:** It might help the reader if you mark the upper and lower layers at least on the y-axis, as you write about the upper layer and the lower layer e.g. line 394, line 397.
Thank you for the comment. We agree that this can be helpful. Instead of marking upper and lower layer in the result plots, we replaced Layer 1 by lower layer and Layer 2 by upper layer in Fig. 3 and changed the names at all relevant locations in the text of the revised manuscript. Furthermore, we improved the figure caption of Fig. 4 to clarify our interpretation of the locations of upper and lower layers in the revised manuscript. In the final manuscript, we will carry over this change to the rest of the figures.
- **Line 420:** You mention that this is explained in detail in Schürholt et al. but a short summary would be helpful. 1 to 2 sentences e.g. why, also in reality? Where observed? Why peak, why peak between layers?
This is clearly an important point! Although some explanations of the sublimation rate peak were already included further down in the section text, we agree that this can be emphasized more: In the revised manuscript, we extended the caption of Fig. 6 and the text to explain that the small peak in deposition rate of (a) (so to the right) is interpreted as the onset of the spatio-temporal oscillations. We also included a short reference to the results of [Schürholt et al. \(2021\)](#) in the revised manuscript.
- **Line 421 – 426:** Very interesting. It would be valuable if you could discuss this further and in relation to reality. What is expected in reality? Why is the peak 4 times higher? We agree that this is interesting. In order to focus more on this discussion, we reorganized the section and included an explanation why sublimation is stronger for the fully coupled processes. Results from an ongoing literature search regarding ranges observed in experiments will be included in the final version of the manuscript.
- **Line 430:** In equation 23 und 24, E_c and E_t are used, but only one number is given here. The meaning of this is unclear. Shouldn't there be one number for E_c and one for E_t ?
You are right, in principle both could be evaluated independently. However, this does not yield additional information, as the deposition rate is directly derived from temperature via the vapor transport equation. Still it might be interesting to look at both due to their non-linear relation.
We replaced 'error term' with 'higher-order mesh errors', as this is the focus of our error analysis. 'error' refers to a quantitative value, whereas the higher-order mesh error terms are a mathematical expression. We determine the error by computing the temperature deviation between the solution that considers higher order mesh error terms, and the solution that doesn't (quantified in an L1 norm). We reformulated the explanation in the revised manuscript. We also added a unit to the error K.
- **Figure 6:** It would be valuable for the work if you also add a plot c) for the temperature gradient for case 5. Perhaps a plot d) for vapour density gradient for case 5 over time would also be beneficial. You write about both in your text.
Thanks for this comment. These additional plots can easily be generated for the final version of the manuscript.

- **Figure 7:** (a) Where is the dashed line? If it coincides with the solid line, please change the visualisation so that both lines are visible.
Indeed, the lines coincide. We will improve their visibility in the final version of the manuscript.
- **Figure 8:** Not mentioned in the text.
Thanks for the comment. Indeed, a reference to the figure was missing in the text. We included a reference in the new subsection **Heat and vapor transport coupled to settling with a dynamic viscosity (Case 4, 6, and 7)** of the revised manuscript (see also response to your major comments on Section 4.6 and Fig. 10). Note that this also led us to change the order of Fig. 8 and 9.
- **Line 441:** I recommend adding at the end of the sentence “for case 7 of Table 2, which refers to the fully coupled process in combination with dynamically varying viscosity”.
We included the reference to Table 2 as suggested.
- **Line 443 – 444:** Please add a discussion why this is the case.
Thanks for the remark. We added a short discussion.
- **Line 449:** “As discussed before” please add section number.
Done!
- **Line 452:** I suggest adding “Figure 10 (a) [...] for case 8”.
We included this comment.
- **Line 458:** “decreases in height”. I recommend providing numbers from what height to what height or by how many cm?
It decreased by 9 cm. We added this detail to the revised manuscript.
- **Line 456:** You use alternately “paper, study and article” in your manuscript. I recommend deciding on one term for the whole manuscript.
We changed it to paper at all relevant locations in the revised manuscript.
- **Line 531:** “in the respective section” Please add section number.
We added the section reference in the revised manuscript.
- **Line 537:** (e.g. Vionnet et al. (2012))
We added brackets to the reference in the revised manuscript.
- **Section 5:** In your summary and conclusion section, you use about one page to write about future work and challenges. I recommend moving this part to a separate section called e.g “Future work and challenges” before the summary and conclusion section.
Thanks for this suggestion. We will reorganize Section 5 and split it into **Future work and challenges** and **Summary and conclusions** in the final version of the manuscript.
- **Line 561:** “Audet and Fowler, 192 please remove brackets.
We removed the brackets accordingly in the revise manuscript.
- **Line 607:** Define ρ_a .
We included a definition for ρ_a in the revised manuscript, and we furthermore added it to Table 1 (see reply to Table 1).

- **Figure D1:** Why are different times shown here than in the other plots (15h, 32 h, 48h vs. 0 h, 16 h, 48h)? I suggest making the graphic square. We will adjust the times of this plot according to the previous plots in the final version of the manuscript.
- **Line 729:** 2021. Thanks for spotting. We corrected the year of the reference in the revised manuscript.

2 Referee#2 comments

Simson et al. present rigorous development of a numerical model for coupled heat transport, vapour diffusion and settling in snow. I expected this to be a difficult paper to read, but I was pleasantly surprised by how readable and understandable it was. Because this is presented as a contribution towards snow model development rather than a full snow model, the test cases that can be considered are necessarily limited, but it is still disappointing that the paper contains no comparisons with observations at all.

2.1 Specific comments listed by Line number

- **Line 2:** The majority of models use non-deforming layers with ice and water moving between them and enforced conservation of mass.
What we meant is the majority of detailed snowpack models. We clarified it in the text of the revised manuscript.
- **Line 18:** Doesn't the focus on snow water equivalent suggest that mass is the most important prognostic variable?
The snow water equivalent is only one of many examples that shows the significance of the snow density.
- **Line 23** Bartelt and Lehning (2002) do use a Lagrangian coordinate system that moves with the ice matrix, but "Lagrangian coordinate system that moves with the ice matrix" is not actually a quote from that paper.
We double checked the quote. It is a quote of the paper by Bartelt and Lehning (2002) (doi:10.1016/S0165-232X(02)00074-5) found on page 127 left column: " A Lagrangian coordinate system that moves with the ice matrix is employed. "
- **Line 57** Considering this motivation from Domine et al., demonstrating whether modelled vapour transport can produce the sort of density stratification observed in shallow Arctic snowpacks subject to high temperature gradients would be an important test case.
Thank you for this suggestion that we take under consideration for a potential comparative study with observational data in the future. Please also see our response to the first major comment of Referee#1.
- **Table 1** c and v are not state variables in the thermodynamic system sense; they can be derived from known temperature, ice volume fraction and vapour density. Excessive precision for latent heat of sublimation
We agree to this comment and corrected the table by moving c and v to the **Model parameters of snow** section in the revised manuscript. Please note, that further changes of Table 1 are due to Referee#1's comment on Table 1.

The constant values are due to Calonne et al. (2014). We converted the latent heat of sublimation from J/m^3 to J/kg . As our computations are based on this latent heat value, we decided to keep the latent heat value in the table but rounded up the decimal.

- **Line 129** Could note that the settling velocity was neglected in Part 1, equation 7
This is a good suggestion that we included in the revised manuscript.
- **Line 216:** Better to write vapour density with the eq subscript hereafter.
We agree with the referee and replaced ρ_v by ρ_v^{eq} in the revised manuscript.
- **Line 220:** Equation 10 differs from the corresponding equation 5 in Part 1. Checking units, the error is actually in Part 1.
Thank your for spotting. We will correct this error in Part 1.
- **Figure 2 caption:** The last three sentences don't really fit in a figure caption.
We agree to this comment and moved the last three sentences to the text of the revised manuscript.
- **Table 2 caption:** Case 8 is also fully coupled.
Thanks for the comment! We added Case 8 as fully coupled in the table caption of the revised manuscript.
- **Figure 3:** Why do the ice volume fraction and temperature axes run right to left?
Thank you for the comment. We agree that direction of the axes does not make sense and changed them to left to right running axes in the revised manuscript. We also changed T_0 to T^0 .
- **Figure 4:** An additional plot with vertical profiles of density at 0, 16 and 48 hours could be interesting. Compaction from 150 to 420 kg/m^3 over 2 days at the base of a 50 cm snowpack seems high if there were to be a comparison with observations (but not as implausible as Figure 10).
Levels on plot (b) appear quantized but the colour bar is not.
We agree with the referee that these plot would be a value-add. These additional plots can easily be generated for the final version of the manuscript. We will also adjust colour levels in (b) for the final version of the manuscript. Regarding the comment on observations please see our reply to Referee#1's for major comment 1. and line 383.
- **Figure 7** Deposition rate would be better shown with a diverging colour scale centred on 0.
This is a good suggestions, thanks! We assume that the referee meant Fig. 6 because Fig. 7 does not have a colour plot, and it does not show deposition rate. We will adjust all color scales for deposition rate to a diverging color scale in the final version of the manuscript.
- **Figure 8:** Reference to Figure 8 is missing in the text. Thanks for the remark. See our reply to to Referee#1 on Fig. 8..
- **Line 470:** A layer-based snowpack model could be viewed as having computational nodes in the centres of the layers. Overburden on the top layer being half the layer's weight then makes more sense. If using Vionnet et al. (2012) as an example, this two-layer, 50 cm snowpack is something that would not arise in Crocus; thin layers are maintained at the top and bottom of the snowpack for heat conduction calculations.
Thank you for this comment. In response to this comment, we suggest to include an additional synthetic test case with thin layers at the top and the bottom of the snowpack to comply

with a more realistic comparison to Crocus. This suggestion is also stated in our reply to major comment 1. of Referee#1. The way our model is setup, we do not intend to place computational nodes at the centre of the layers since the nodes rather constrain the extent of the individual numerical layers.

- **Line 594:** a_0 , a_1 , a_2 and f all have units, which should be given. f is the gas constant for water vapour. This same formula was attributed to Mason (1971) in Part 1.
Thanks for the remark. We added the units.

Minor corrections: Thanks for spotting! We included all of the following minor corrections in the revised manuscript.

- **Line 25:** “has been well established”
- **Line 56:**
“Both require”
- **Line 57:** “uses time steps on the order of 15 minutes or longer”
- **Line 74:** “do not take full advantage”
- **Line 157:** “depends on both the physical regime and computational feasibility”
- **Line 161:** “challenging to determine from experiments”
- **Line 197:** “In the remainder of this paper”
- **Line 244:** “results in the necessary accuracy”
- **Line 253:** “implemented in Python”
- **Line 254:** “but also allows”
- **Line 305:** “avoids numerically approximating”
- **Line 309:** The lengthy parenthetical clause “see for instance Sect. 3.4. in Bartelt and Lehning (2002) or its recent extension Jafari et al. (2020)” would be better inside parentheses than between commas.
- **Line 317:** “allows inferring the most plausible process model ... given certain data”
- **Line 319:** “results in a mesh”
- **Line 530:** “without conceptual difficulty”
- **Line 568:** “While including potential phase changes”
- **Line 598:** Part 1 used capital Theta for the Heaviside function.
- **Line Appendix C:** Matrix elements should be enclosed in brackets.

3 Additional typo correction based on our own review

For completeness, we also list minor typo-like changes that we implemented in the revised version of the manuscript. Note, that none of these changes affect the results.

- **line 297**: We changed the definition of the cell sizes Δz_j to $\Delta z_j := z_{j+1} - z_j$ with $j \in [0, nz[$ to respect that the number of cells nc is always the number of nodes nz minus 1.
- **Eq. (13), (14)**: minus instead of plus in front of $\partial_z v \phi_i$
- **Eq. (19)**: k instead of l in the sum index
- **Eq. (21)**: derivative of temperature w.r.t. time instead of temperature
- **Eq. (22)**: added latent heat L to α_T and k_{eff} to β_T
- **Eqs. (23), (B1), (B2)**: added superscript n to Δz_{k-1}^n
- **Eq. (C8)**: added subscript c to $\alpha_{c,k}$
- **Eqs. (C11), (C8)**: Division by Δt^n .

References

- Brun, E., Martin, E., Simon, V., Gendre, C., and Coleou, C.: An Energy and Mass Model of Snow Cover Suitable for Operational Avalanche Forecasting, *Journal of Glaciology*, 35, 333–342, <https://doi.org/10.3189/s0022143000009254>, 1989.
- Calonne, N., Geindreau, C., and Flin, F.: Macroscopic Modeling for Heat and Water Vapor Transfer in Dry Snow by Homogenization, *The Journal of Physical Chemistry B*, 118, 13393–13403, <https://doi.org/10.1021/jp5052535>, 2014.
- Domine, F., Picard, G., Morin, S., Barrere, M., Madore, J.-B., and Langlois, A.: Major Issues in Simulating Some Arctic Snowpack Properties Using Current Detailed Snow Physics Models: Consequences for the Thermal Regime and Water Budget of Permafrost, *Journal of Advances in Modeling Earth Systems*, 11, 34–44, <https://doi.org/10.1029/2018ms001445>, 2019.
- Hansen, A. and Foslien, W.: A macroscale mixture theory analysis of deposition and sublimation rates during heat and mass transfer in dry snow, *The Cryosphere*, 9, 1857–1878, <https://doi.org/10.5194/tc-9-1857-2015>, 2015.
- Jafari, M., Gouttevin, I., Couttet, M., Wever, N., Michel, A., Sharma, V., Rossmann, L., Maass, N., Nicolaus, M., and Lehning, M.: The Impact of Diffusive Water Vapor Transport on Snow Profiles in Deep and Shallow Snow Covers and on Sea Ice, *Frontiers in Earth Science*, 8, 249, <https://doi.org/10.3389/feart.2020.00249>, 2020.
- LeVeque, R. J.: *Finite Volume Methods for Hyperbolic Problems*, Cambridge Texts in Applied Mathematics, Cambridge University Press, <https://doi.org/10.1017/CBO9780511791253>, 2002.
- Schweizer, J., Jamieson, J. B., and Schneebeli, M.: Snow avalanche formation, *Reviews of Geophysics*, 41, 1016, <https://doi.org/10.1029/2002rg000123>, 2003.
- Schürholt, K., Kowalski, J., and Löwe, H.: Elements of future snowpack modeling - part 1: A physical instability arising from the non-linear coupling of transport and phase changes, *The Cryosphere*, <https://doi.org/10.5194/tc-2021-72>, companion paper, 2021.

- Viallon-Galinier, L., Hagenmuller, P., and Lafaysse, M.: Forcing and evaluating detailed snow cover models with stratigraphy observations, *Cold Regions Science and Technology*, 180, 103 163, <https://doi.org/10.1016/j.coldregions.2020.103163>, 2020.
- Vionnet, V., Brun, E., Morin, S., Boone, A., Faroux, S., Moigne, P. L., Martin, E., and Willemet, J.-M.: The detailed snowpack scheme Crocus and its implementation in SURFEX v7.2, *Geoscientific Model Development*, 5, 773–791, <https://doi.org/10.5194/gmd-5-773-2012>, 2012.
- Wever, N., Valero, C. V., and Fierz, C.: Assessing wet snow avalanche activity using detailed physics based snowpack simulations, *Geophysical Research Letters*, 43, 5732–5740, <https://doi.org/10.1002/2016GL068428>, 2016.

Elements of future snowpack modeling - part 2: A modular and extendable Eulerian–Lagrangian numerical scheme for coupled transport, phase changes and settling processes

Anna Simson¹, Henning Löwe², and Julia Kowalski^{1,3}

¹AICES Graduate School, RWTH Aachen University, Schinkelstr. 2a, 52062 Aachen, Germany

²WSL Institute for Snow and Avalanche Research SLF, Flüelastr. 11, 7260 Davos, Switzerland

³Computational Geoscience, Geoscience Centre of the University of Göttingen, Goldschmidtstr. 1, 37077 Göttingen, Germany

Correspondence: Anna Simson (simson@aices.rwth-aachen.de)

Abstract. A coupled treatment of transport processes, phase changes and mechanical settling is the core of any detailed snowpack model. A key concept underlying the majority of [these](#) models is the notion of layers as deforming material elements that carry the information on their physical state. Thereby an explicit numerical solution of the ice mass continuity equation can be circumvented, however at the downside of virtual no flexibility in implementing different coupling schemes for densification, phase changes and transport. As a remedy we consistently recast the numerical core of a snowpack model into an extendable Eulerian–Lagrangian framework for solving the coupled non-linear processes. In the proposed scheme, we explicitly solve the most general form of the ice mass balance using the method of characteristics, a Lagrangian method. The underlying coordinate transformation is employed to state a finite-difference formulation for the superimposed (vapor and heat) transport equations which are treated in their Eulerian form on a moving, spatially non-uniform grid that includes the snow surface as a free upper boundary. This formulation allows to unify the different existing view points of densification in snow or firn models in a flexible way and yields a stable coupling of the advection-dominated mechanical settling with the remaining equations. The flexibility of the scheme is demonstrated within several numerical experiments using a modular solver strategy. We focus on emerging heterogeneities in (two-layer) snowpacks, the coupling of (solid-vapor) phase changes with settling at layer interfaces and the impact of switching to a non-linear mechanical constitutive law. Lastly, we discuss the potential of the scheme for extensions like a dynamical equation for the surface mass balance or the coupling to liquid water flow.

Copyright statement.

1 Introduction

The snow density is probably the most important prognostic variable of any snowpack model as e.g. reflected by a focus on snow water equivalent in past snow model intercomparison projects (Krinner et al., 2018, and references therein). That said, it actually comes as a surprise when not even the detailed snowpack models, [e.g. Crocus and SNOWPACK](#), explicitly state

an ice mass conservation equation in their technical documentation (Brun et al., 1989, 1992; Lehning et al., 2002; Bartelt and Lehning, 2002). Only a more detailed inspection reveals how mass conservation is accounted for, namely rather indirectly by stating a settling law for individual layers and resorting to a “Lagrangian coordinate system that moves with the ice matrix” (Bartelt and Lehning, 2002) to translate the ice phase deformation into a thickness evolution of the layers (Brun et al., 1989; Vionnet et al., 2012). While this procedure is has been well established for a long time, it is without numerical ambiguities only in the absence of phase changes. In addition, this non-explicit nature of the most important conservation law in snow makes it virtually impossible to isolate and advance the numerical core of a snowpack model as an encapsulated numerical scheme comprising all involved coupled non-linear partial differential equations.

This non-explicit treatment of snow density or ice mass continuity in snowpack models, e.g. SNOWPACK and Crocus, has to be contrasted to other existing work on densification, comprising both, stand-alone numerical snow studies (Meyer et al., 2020) and the vast body of work on firn densification (Lundin et al., 2017). All of the latter models are built around an explicit formulation of the ice mass continuity equation. This conceptual difference renders a general comparison of firn and snow densification mechanisms (Lundin et al., 2017) difficult. For model intercomparisons in the future it is thus desirable to have a numerical core that is able to digest arbitrary snow or firn densification physics, with a flexible but rigorous coupling to superimposed non-linear transport and phase change processes.

Any holistic snowpack model has to account for transport of heat, vapor and liquid water, its induced phase change processes, as well as mechanical settling and apparent metamorphic processes on the snow’s microstructure. A widespread body of literature exists that proposes different modeling approaches and computational tools for the various flavors and perspectives of this multi-physics coupled situation, e.g. Krinner et al. (2018, and references therein). For the general timescales of interest (diurnal up to seasonal), it is common practice to employ a continuum assumption and to model the snowpack’s state as a mixture of ice, vapor, water and air, as initially described in Bader and Weilenmann (1992). Detailed snowpack models, such as SNOWPACK (Lehning et al., 2002) and CROCUS (Vionnet et al., 2012) are built upon this type of mixture theoretical approach and used for a wide range of purposes.

While heat transport, mechanical settling and processes due to the presence of liquid water have been incorporated into SNOWPACK (Bartelt and Lehning, 2002) and CROCUS (Vionnet et al., 2012) for a long time, effects due to vapor transport have mostly recently been investigated in separate studies. Temperature gradients between ground and atmosphere imply upward vapor fluxes in snowpacks. Stronger temperature gradients (either due to a smaller snowpack height or colder surface temperature) in the Arctic yield higher vapor fluxes (Domine et al., 2019) compared with alpine snowpacks. Depth hoar layer with reduced density and thermal conductivity form at the snowpack’s bottom. In alpine snowpacks similar hoar layers develop within the snowpack that may cause avalanches due to their low mechanical stability (Schweizer et al., 2003). Upscaled and homogenized continuum mechanical process models that account for vapor transport are, for instance, put forward by Hansen and Foslien (2015) and Calonne et al. (2014). Both couple the snowpack’s evolving temperature profiles to a non-linear reaction-diffusion type of equation for vapor transport and phase change. While they provide different flavors of how to set up the underlying mathematical model, both approaches are formulated for idealized conditions and investigate vapor diffusion in the absence of settling and therefore neglect its feedback on the apparent snow density. These model-based investigations, but

also field-based observations in arctic snowpacks on top of permafrost (Domine et al., 2016, 2019) demonstrated the significance of vapor related processes in snow. Hence, it is of great interest to investigate further, how vapor interacts with apparent mechanical processes within the snowpack.

Incorporating vapor transport directly into a fully coupled snowpack model is however challenging, e.g. due to the fact that the associated characteristic time scales are small, and expected effects on the snowpack are localized ~~Both requires~~ (Schürholt et al., 2020, 2021). Both require a much higher spatio-temporal resolution than typically provided by existing operational schemes. In its original version, SNOWPACK for instance uses time steps ~~in-on~~ the order of 15 min or larger (Bartelt and Lehning, 2002) to facilitate seasonal simulation times. For Crocus time steps are on the order of 15 min (Viallon-Galinier et al., 2020) to 1 hour (Vionnet et al., 2012). The recent work of Jafari et al. (2020) provides a first attempt to account for vapor transport within a coupled snowpack model. In their paper, they accounted for diffusive vapor transport and phase change following Hansen and Foslien (2015) and analyzed its feedback on the snow density. In order to resolve diffusive processes, simulations were conducted at much shorter time steps of 1 min and a finer spatial resolution at approximately 0.1 cm. ~~While this~~ For comparison, a typical layer thickness in SNOWPACK is 2 cm (Wever et al., 2016) and the minimum layer thickness in Crocus is 0.5 cm (Brun et al., 1989). While Jafari et al. (2020)'s work demonstrates the general feasibility of vapor-coupled snowpack models, the exact nature of how vapor transport and phase changes interfere with stress-induced settling remains to be investigated in-depth.

It is well known that any numerical strategy that aims at simulating simultaneous settling-induced deformation of the snowpack and (arbitrary) diffusive transport requires a special computational treatment to couple both. Diffusive transport and reactive phase change is best modelled by taking a Eulerian perspective, hence on a static mesh. In contrast there exist a number of different techniques to incorporate the settling induced deformation. One option is to use a time-dependant coordinate transformation by Morland (1982), who developed a fixed domain transformation to solve one-phase diffusion problems with a moving free surface on a finite, time-invariant computational domain. An alternative approach was put forward by Wingham (2000), who used a different spatio-temporal coordinate transformation for firn densification. Both transformation strategies effectively eliminate the vertical motion (or gradients of it) from the computational update procedure. And exactly the same is (implicitly) done in the present treatment of densification in snowpack models (Bartelt and Lehning, 2002; Vionnet et al., 2012), where the coordinate transformation embodied in deformation of the underlying computational grid through the update of layer positions/thicknesses is (implicitly) exploited for the ice mass conservation. However, the present descriptions do not take the full advantage of a clear and explicit separation into a Lagrangian deformation module that accounts for mechanical settling and a Eulerian transport and phase change module. The benefit of this hybrid computational strategy is that it is easy to understand, computationally feasible, provides a modular error control and increases the interpretability by disentangling numerical artefacts from features of the underlying non-linear process models. Hybrid numerical schemes that combine an Eulerian process model with a Lagrangian-type spatio-temporal mesh adaptation are not new and have been used in other disciplines, e.g. for phase change problems (Lacroix and Garon, 1992), as σ -coordinates in oceanography, where the ocean's surface and bottom are projected on coordinates $\sigma = 0$ and $\sigma = -1$ that follow the ocean floor's topography (Mellor and Blumberg, 1985), or for shallow flow models (Kowalski and Torrilhon, 2019).

The aim of our work is twofold: First, we will describe our numerical strategy for a phase-changing snowpack. The numerical scheme is hybrid, in the sense that it clearly discriminates between a solution of the mechanical settling operator by means of a Lagrangian approach and a solution to the transport and phase change operator by means of an Eulerian approach. To some degree, the numerical model description must be understood as a rigorous re-formulation of the numerical schemes from existing computational snowpack models. Yet, in addition to existing schemes we a) explicitly separate the Eulerian and Lagrangian part of the solver to facilitate a later modular adaption, b) provide a full finite difference formulation including correction terms due to the deforming (non-uniform) mesh that are typically omitted and c) discuss options to increase the approximation accuracy of the various parts of the numerical scheme. Second, we demonstrate the computational potential by applying and analyzing simulation results for an idealized two-layer, dry snow situation. We consider a model cascade of different process building blocks, which in their most comprehensive version, correspond to fully coupled heat and vapor transport alongside phase changes and settling.

With this work we seek to contribute to anticipated future developments of snow or firn models, or likewise extensions of existing ones, that aim at flexibility and modularity, while providing a simple, mathematically rigorous numerical approximation for a stable and robust integration of generic multi-physics process equations. By modularity and extendability we understand the possibility to consider or neglect specific process modules and parametrizations in a straight-forward way. This modularity would enable to a) investigate competing non-linear effects systematically from a cascade of process models, b) assess the quality of the numerical approximation independently and c) conduct a standardized model selection based on well-defined benchmarks.

The [article paper](#) is structured as follows. In Sect. 2, we recall the dry snow model equations comprising the relevant transport, phase change and mechanical aspects. In Sect. 3, we introduce the Eulerian-Lagrangian numerical scheme and its solution using the method of characteristics. In Sect. 4, we present and discuss results from a number of simulation scenarios, including verification scenarios that consider transport, phase changes, and mechanics in the absence of any interaction, as well as coupled scenarios that focus on their interplay. We furthermore investigate the impact of different viscosity parametrizations and assess the behavior when switching to a Glen-type of non-linear constitutive closure. Finally, we compare our results to a conventional layer-based treatment. In Sect. 5, we summarize and discuss our findings, and draw conclusions towards future snowpack modeling.

2 Physical model

2.1 General situation

As a common starting point, snow models take a macroscale perspective that volume-averages [\(Bartelt and Lehning, 2002; Bader and Weilenmann, 1992; Hansen and Foslien, 2015\)](#) or homogenizes [\(Calonne et al., 2014\)](#) the snowpack's microstructural state into macroscale variables. If not stated otherwise, we implicitly assume all state variables to be macroscale variables ~~without explicitly mentioning it every time~~. State variables, model parameters and constants used in this paper are summarized in Table 1.

In the most general case, snow is a mixture of ice, air, vapor and water, and the snow density is given as a mixture of the respective pure densities (Bader and Weilenmann, 1992; Morland et al., 1990). The amount of ice within in one reference volume is referred to the ice volume fraction of snow is $\phi_i \rho_i V$, in which ϕ_i which for dry snows related to denotes the ice's volume fraction, ρ_i its pure density, and V the volume of the reference volume. For dry snow, further contributions due to water can be neglected, and the snow density by can be approximated as $\phi_i \rho_i$ with ρ_i ice density. In a general snowpack, the ice matrix's void space $1 - \phi_i$ is filled to different degrees with air, vapor, or even water. Structure and volume fraction of the ice can change over time either due to strain-induced settling processes, or due to transient phase changes, such as sublimation and deposition or melting and freezing. Our study paper focuses on the derivation of a hybrid Eulerian-Lagrangian framework to solve settling, transport and phase changes with an assessment of the computational building blocks. To this end we restrict ourselves to dry snow and allow for one secondary phase (vapor) in a Eulerian treatment coupled to the Lagrangian treatment of the ice phase. With respect to computational model development, we regard the dry snow situation as the more challenging (yet less investigated) one compared to the wet snow situation, mostly due to a broader spectrum of characteristic spatial and temporal scales involved (see more detailed discussion in Sect. 5).

Note, that water transport and solid-liquid phase change can in principle be integrated following a similar strategy presented in this paper. The following section introduces the (macroscale) snowpack model where the subsection structure reflects the later described modular structure of the numerical core.

2.2 Ice mass balance

The ice volume fraction $\phi_i = \phi_i(\mathbf{z}, t)$ within a spatio-temporally evolving snowpack of varying snow height $H(t)$ is governed by the ice mass balance and reads

$$\partial_t \phi_i + \nabla \cdot (\mathbf{v} \phi_i) = \frac{c}{\rho_i}, \quad (1)$$

with velocity field \mathbf{v} , source term c , and intrinsic ice density ρ_i (Hansen and Foslien, 2015; Bader and Weilenmann, 1992). Note that mechanical settling is neglected in Part 1 of this companion paper. The corresponding ice mass balance (Eq. 7 in Part 1) does thus not include the velocity field \mathbf{v} .

In a 1d situation that focuses on an evolving vertical snow column, we have vertical position z as the only relevant spatial coordinate ($z \in [0, H(t)]$). The velocity field \mathbf{v} reduces to vertical velocity $v = v(z, t)$ that depends on time and position within the column. It is negative for snow height decrease and positive for snow height increase. Vertical motion results either from mechanical settling, hence a consolidation or compaction of the snowpack, or alternatively it is a continuity response to changes in ice volume from sublimation/deposition, which or melting/freezing via the source term c . The continuity response leads to a minor vertical decrease/increase of snow height. Though effects due to consolidation of snow may be significantly more pronounced than those due to phase change processes in the pore space, the latter needs to be accounted for to acknowledge mass conservation of the complete system. At this point in time, we do not consider any additional increases of snow height due to precipitation, yet we discuss how this can be included in the future in Sect. 5.

The source term $c = c(z, t)$ varies with time and position in the column and stands for a gain or loss of ice mass from phase

Table 1. Terminology of state variables, model parameters and constants

Symbol	Name	Equation/Value	Unit
State variables			
ϕ_i	Ice volume fraction	Eq. (1)	–
ρ_v	Vapor density	Eq. (A1)	kg m^{-3}
T	Temperature	Eq. (11)	K
Model parameters of snow			
v	Vertical velocity	Eq. (7)	m s^{-1}
c	Ice deposition rate	Eq. (9)	$\text{kg m}^{-3} \text{s}^{-1}$
$\dot{\epsilon}$	Strain rate	Eq. (3)	s^{-1}
η	Viscosity	Eq. (4)	Pa s
σ	Stress	Eq. (5)	Pa m^{-2}
ρ_{snow}	Density	Eq. (5)	kg m^{-3}
D_{eff}	Vapor diffusion coefficient	Eq. (A2)	$\text{m}^2 \text{s}^{-1}$
$(\rho C)_{eff}$	Heat capacity	Eq. (A4)	$\text{J m}^{-3} \text{K}^{-1}$
k_{eff}	Thermal conductivity	Eq. (A3)	$\text{W m}^{-1} \text{K}^{-1}$
Parameters assumed to be constant (Calonne et al., 2014)			
ρ_i	Ice density $\phi_i = 1$	917	kg m^{-3}
L	Ice latent heat of sublimation	2835333	J kg^{-1}
C_i	Ice heat capacity $\phi_i = 1$	2000	$\text{J kg}^{-1} \text{K}^{-1}$
ρ_a	Air density $\phi_i = 0$	1.335	kg m^{-3}
C_a	Air heat capacity $\phi_i = 0$	1005	$\text{J kg}^{-1} \text{K}^{-1}$

change (Bader and Weilenmann, 1992) per unit volume and unit time. ~~It~~ As we constrain this paper on the dry situation we will henceforth refer to c as the deposition rate. c is positive (production) if new ice is built, hence vapor deposits, and it is negative (loss) if ice is lost, hence sublimates. ~~Henceforth we will refer to e as the deposition rate.~~ Finally, ρ_i denotes the constant intrinsic density of ice and serves as a scaling factor. The ice mass balance (Eq. (1)) couples mechanical settling and phase change processes. Considering the equation in its full form is essential for our goal to model and eventually analyze the interplay between these processes. The structure of the ice mass balance resembles an advection-reaction equation that can conveniently be solved by means of Lagrangian type computational methods, such as the method of characteristics (see Sect. 3). Yet in order to do so, we need to provide a closure for both vertical velocity v and deposition rate c .

165 2.3 A closure for the velocity field

Velocity v represents mechanical deformation in the snowpack. Its idealized relation to the strain rate is given by

$$\nabla v = \dot{\epsilon}, \tag{2}$$

Note that this is simplified with respect to more general, tensorial formulations of 1d consolidation theories, see for instance Audet and Fowler (1992). Yet even the idealized formulation Eq. (2) will be sufficient for our purposes, as it resembles the
 170 approach ~~typically implicitly~~ chosen in snowpack models ([Bartelt and Lehning, 2002](#); [Vionnet et al., 2012](#)).

In general one would expect that porous snow inherits the non-linear constitutive behavior of ice (Kirchner et al., 2001), which leads to

$$\dot{\epsilon} = \frac{1}{\eta} \sigma^m, \quad (3)$$

which is a variant of Glen's law. Here, η denotes the compactive viscosity of snow and σ denotes the stress. The choice of the
 175 Glen exponent m in earlier work depends on both the physical regime ~~but also on and the~~ computational feasibility. The linear form of Glen's law ($m = 1$) is chosen in Vionnet et al. (2012) and Bartelt and Lehning (2002). For the sake of comparability we thus mainly use a linear version of Glen's law, hence $m = 1$. Our framework, however, also copes with the non-linear relation, such as $m = 3$, and we later include a comparative example.

The compactive viscosity η depends on the snow's microstructure and is challenging to ~~be determined~~ [determine](#) from exper-
 180 iments (Wiese and Schneebeli, 2017). It is typically provided as a parametrized closure for a specific physical situation and strongly correlates with the choice for the Glen exponent m . This fact clearly constrains its universal applicability and makes any transfer of a validated snowpack model to other physical situations challenging. In this article, we will consider both constant viscosity scenarios, as well as an additional scenario with a varying viscosity assuming an empirical viscosity closure from Vionnet et al. (2012)

$$185 \quad \eta(\phi_i, T) = f \eta_0 \frac{\rho_i \phi_i}{c_\eta} \exp(a_\eta (T_{ph} - T) + b_\eta \rho_i \phi_i), \quad (4)$$

with state variables temperature T and ice volume fraction ϕ_i and constants ice density ρ_i , phase change temperature $T_{ph} = 273$ K and further constants $\eta_0 = 7.62237 \times 10^6$ kg s⁻¹, $a_\eta = 0.1$ K⁻¹, $b_\eta = 0.023$ m³ kg⁻¹, $c_\eta = 250$ kg m⁻². Finally, f reflects properties of the snow microstructure ~~and i.e. the angularity and the size of the grains, and it and~~ is assumed to be 1 in our case. The constant viscosity value applied to linear Glen's law $\eta_{const, m=1}$ is derived with intermediate values for
 190 ice volume fraction and temperature of the respective initial conditions. These values are plugged into the empirical closure Eq. (4) to solve for viscosity. The same procedure cannot be applied to derive a constant viscosity value for the non-linear version of Glen's law $\eta_{const, m=3}$ since the viscosity closure (Eq. (4)) has initially been calibrated to the linear form of Glen's law ($m = 1$). Instead we choose a snow deformation rate from the literature ($\dot{\epsilon} = 10^{-6}$ s⁻¹ (Johnson, 2011)) and determine the maximum stress value from the initial snow density. These strain rate and stress values are then inserted into the constitutive
 195 relation (Eq. (3)) which is finally solved for viscosity. To avoid infinite ice volume growth above physical values ($\phi_i > 1$) the viscosity must tend to infinity for $\phi_i \rightarrow 1$. Therefore, the constant viscosity values are restricted to ice volumes below 0.95 by multiplication with an ice volume fraction dependent power law (Appendix (A6)). This power law yields ≈ 1 for $\phi_i \leq 0.95$ and exponentially increases for higher ice volumes. Multiplied with the constant viscosity values viscosity remains constant below $\phi_i < 0.95$ and exponentially increases above, which stops further densification and settling. This procedure does not intend to
 200 reproduce the correct physics for low porosity ice, which mathematically leads though to a similar crossover behavior.

In the absence of strong horizontal deformation and deviatoric stress components, it is reasonable to assume a stress-free condition at the snow's surface and a hydrostatic stress condition in its interior:

$$\nabla\sigma = g\rho_{eff\,snow}. \quad (5)$$

205 Here, ρ_{eff} is the gravitational acceleration and ρ_{snow} refers to the snowpack's effective snow's density, which is clearly dominated by the ice fraction via $\rho_{eff} \approx \phi_i(z)\rho_i$ and $\rho_{snow} \approx \phi_i(z)\rho_i$. It varies with the position z in the snow column due to a vertically varying ice volume fraction $\phi_i(z)$. Integration of Eq. (5) and combination with Eqs. (2) and (3) yields an expression for the velocity gradient:

$$\partial_z v = \frac{1}{\eta} \left(g \int_z^{H(t)} \phi_i(\zeta) \rho_i d\zeta \right)^m. \quad (6)$$

210 ζ is the integration variable. A second integration along the vertical axis finally yields an expression for the velocity at position z in the snow column:

$$v(z) = - \int_0^z \frac{1}{\eta} \left(g \int_{\tilde{z}}^{H(t)} \phi_i(\zeta) \rho_i d\zeta \right)^m d\tilde{z}, \quad (7)$$

in terms of total height $H(t)$, ice volume fraction $\phi_i(z, t)$, and with $v(z = 0, t) \equiv 0$. This definition of the vertical velocity yields a process that complies with the obvious physical constraints: a) the velocity vanishes at the bottom of the snow column, hence prevents artificial penetration into the ground. This is similar to displacement requirements in SNOWPACK (Bartelt and 215 Lehning, 2002). b) the vertical velocity accumulates with height, which prevents any artificial disaggregation of the snowpack, and c) the vertical velocity relaxes towards zero as the ice volume fraction tends towards its maximum volume fraction $\phi_i < \phi_{i,max} < 1$. In the ongoing-remainder of this paper, we will use Eq. (7) to account for the mechanical settling of the snowpack.

2.4 Transport and phase changes

The ice deposition rate c as relevant to solve Eq. (1) typically depends on a cascade of coupled heat and mass transport for the 220 involved phases ice, water and vapor. In this article, we will consider a process model proposed by Hansen and Foslien (2015) that reflects a dry snow condition in which void space is filled by vapor only. Note, however, that this coupled process model could readily be substituted or extended by another one, e.g. ~~the one from Calonne et al. (2014)~~ from Calonne et al. (2014), Jafari et al. (2020) or Schürholt et al. (2020, 2021).

225 Next, we state the essential aspects and process equations of the model proposed in Hansen and Foslien (2015). ~~We extend the model for mechanics~~ and describe how it can be used to recover the ice deposition rate:

Assuming dry snow conditions, the ice production is solely determined by mass transport between vapor and ice. The vapor mass balance reads

$$\partial_t(\rho_v(1 - \phi_i)) - \nabla \cdot (D_{eff} \nabla \rho_v) + \rho_v \nabla \cdot v \phi_i = -c, \quad (8)$$

in which ρ_v denotes the vapor density and D_{eff} the effective vapor diffusion coefficient. Note that the convective term on the
 230 left hand side derives from mechanical settling and is thus not included in Hansen and Foslien (2015). Its effect on deposition
 rate is rather low, and thus it is neglected in the following. Vapor production corresponds to negative ice deposition rate $-c$
 that represents sublimation. Following Hansen and Foslien (2015), vapor density in the pore space can be assumed to be at
 saturation density ρ_v^{eq} , so that $\rho_v \equiv \rho_v^{eq}$. The latter is well investigated, and empirical relations exist that specify its temperature
 dependency $\rho_v^{eq}(T)$. In this work, we will employ an empirical relation from Libbrecht (1999). The full expression can be read
 235 in Appendix A1. ~~Instead of following the approach of Hansen and Foslien (2015) one could also use another closure for the~~
~~source term (Calonne et al., 2014; Jafari et al., 2020; ?).~~ Due to the closure for vapor density $\rho_v \rho_v^{eq}$, the vapor mass balance
 (Eq. (8)) can be rewritten using the temperature dependence of the equilibrium vapor density

$$(1 - \phi_i) \frac{d\rho_v}{dT} \frac{d\rho_v^{eq}}{dT} \partial_t T - \nabla \cdot \left(D_{eff} \frac{d\rho_v}{dT} \frac{d\rho_v^{eq}}{dT} \nabla T \right) = -c. \quad (9)$$

Assuming the snow to be in thermal equilibrium at the microscale, we can likewise write the energy balance in terms of the
 240 temperature, which reads

$$(\rho C)_{eff} \partial_t T - \nabla \cdot (k_{eff} \nabla T) = cL. \quad (10)$$

The parameters $(\rho C)_{eff}$ and k_{eff} stand for the effective heat capacity of snow and effective thermal conductivity, respectively.
 Both parameters depend on the ice volume fraction, and their definition is stated in Appendix A2. The right hand side of the
 heat equation accounts for latent heat release, which is coupled to phase change processes.
 245 The system of the two equations, Eqs. (9) and (10), and the two unknowns, temperature T and deposition rate c , is solved by
 replacing c in Eq. (10) with Eq. (9), which yields a non-linear equation for temperature

$$\left((\rho C)_{eff} + (1 - \phi_i) \frac{d\rho_v(T)}{dT} \frac{d\rho_v^{eq}(T)}{dT} L \right) \partial_t T = \nabla \cdot \left(\left(L D_{eff} \frac{d\rho_v(T)}{dT} \frac{d\rho_v^{eq}(T)}{dT} + k_{eff} \right) \nabla T \right). \quad (11)$$

The spatio-temporal temperature evolution is then used to recover the ice deposition rate c from either Eq. (9) or Eq. (10).

3 Computational Approach

250 The complete process model is now given by the ice mass balance Eq. (1), its mechanically induced vertical velocity Eq. (7),
 and the coupled system for temperature Eq. (11) and ice deposition rate determined by either Eq. (9) or Eq. (10). Each of the
 equations will be solved in a separate module. The ice mass balance in conjunction with the vertical velocity has the form
 of a non-linear advection equation, whereas the remaining equations are of parabolic nature, which is reflected in our general
 approach to solve the system.

255 3.1 General approach to the computational strategy

Based on the distinction into diffusion and advection dominated processes, we propose a two-step solution scheme:

Step 1 accounts for the mesh deformation and solves the advection dominated mechanical settling, i.e. the ice mass balance Eq. (1), by means of a Lagrangian approach [that tracks the movement of the coordinates including changes from metamorphism](#), and

Step 2 determines the spatio-temporal evolution of temperature and deposition rate fields as introduced in Sect. 2.4 based on an Eulerian approach that solves the diffusion dominated transport and phase changes via a finite difference implementation on a deformed (unstructured) mesh.

Note that here, we employed a finite difference method because it provides a feasible algorithm that ~~results at the necessary accuracy for the~~ [is applicable to the](#) scenarios considered in the paper [using a 1d snow column](#). It also naturally integrates with the Lagrangian part of the solution (Step 1), as we can re-use the same mesh. In principle, it is also possible to couple the two-step approach with a finite element solution for temperature and deposition rate, ~~e.g. for instance~~ when aiming for a 2d or 3d model in a complex geometry ~~. In that situation~~ [that incorporates realistic mountain slope topographies. When using a finite element solver](#), however, we have to keep in mind that deposition rate and temperature fields need to be reconstructed from ~~a finite element~~ [the](#) solution at each time step. Especially when wanting to use higher order elements this might limit computational feasibility.

Our solution scheme alternates both steps via straightforward first order operator splitting. This is found to work well for our simulation scenarios, yet could be readily exchanged with a higher order splitting scheme, e.g. a second order Strang splitting [\(LeVeque, 2002\)](#), if required.

The computational model is implemented ~~into~~ [in](#) Python and it is modular and extendable, in the sense that each module can separately be activated and deactivated. This not only simplifies the verification of individual process building blocks, yet it also allows an in-depth investigation of the various coupling effects and the model's non-linear feedback. Alternative formulations e.g. of the parametrized velocity field are implemented and can easily be exchanged. Finally, the modular structure facilitates the implementation of additional closure relations or the integration of entire new process modules.

3.2 Computational grid

In this [study paper](#), we consider a 1d snow column, which is discretized into $nz + 1$ spatial mesh nodes denoted by z_k with $k \in \{0, 1, \dots, nz\}$. We applied 101 computational nodes ($nz = 100$) except for some simulations that required a higher resolution of 251 nodes ($nz = 250$). The mesh is non-uniform in general, meaning that the distance between neighboring nodes $z_{k+1} - z_k$ varies throughout the snow column and with time. Note that the axis is oriented opposing gravitational acceleration, such that z_0 denotes the position of the ground and z_{nz} the position of the snowpack's free surface. Time increments are denoted by t_n with $n \in \{0, 1, \dots, nt\}$ and nt being the maximum number of time steps in a complete simulation run. For each of the field variables subscript k denotes the vertical coordinate and superscript n denotes the time step hence $T(z_k, t_n) = T_k^n$.

290 **3.3 Lagrangian solution of the ice mass balance**

When the snowpack is subject to vertical motion, e.g. settling, its physical height decreases, hence its vertical extent shrinks. One option to reflect this in a computational method is to adjust the spatial node coordinates accordingly. The challenging fact in our situation is that the vertical motion within the snow column (non-linear advection) is coupled to phase changes, i.e. a change in ice volume fraction via the source term in the ice mass balance (Eq. (1)). The method of characteristics is a suitable
 295 method to solve such a non-linear advection equation with source term. It can be interpreted as a simultaneous motion tracking of snow material elements or "particles", referred to as the integration along so-called characteristics, while also accounting for its metamorphism along the trajectory. By construction, the method correctly tracks the snowpack's moving free surface. Due to the fact that the snow column's evolution is determined with respect to a material particle that moves vertically at speed v in the snowpack, the method of characteristics is called a Lagrangian approach.

300 In order to derive the specific update rule for the ice mass balance Eq. (1), we first apply the chain rule to its initial Eulerian version

$$\partial_t \phi_i + v \partial_z \phi_i = \frac{1}{\rho_i} c - \phi_i \partial_z v \phi_i \quad (12)$$

and then re-formulate the equation in a Lagrangian reference frame, hence with respect to nodes moving at the vertical velocity v . Changing to the moving reference frame effectively compensates the advection term in Eq. (12) and yields

305
$$\partial_t \phi_i = \frac{1}{\rho_i} c \pm \phi_i \partial_z v \phi_i \quad (13)$$

$$\partial_t z = v. \quad (14)$$

Equation (14) accounts for the settling of material particles within the snowpack. We will use it to update the coordinates of the mesh nodes directly, which results in a continuous mesh deformation as illustrated in Fig. 1. Equation (13) captures the evolution of the ice volume fraction along the trajectory of a moving ice material particle within the snowpack. It accounts for
 310 volume changes due to a) mass production/loss in response to phase changes, and b) vertical variation of the vertical velocity. Further details and generalizations of the method of characteristics can be found in Farlow (1993).

Equations (13) and (14) can be solved analytically for a constant vertical velocity and deposition rate. In our case however, the velocity closure is provided by Eq. (7) and the deposition rate results from solving yet another process model (Eqs. (10) and (11)), which requires a numerical solution. Since we expect the response of the ice volume fraction to be slow (with respect to
 315 other processes in the system), we will rely on a first order explicit Euler time integration scheme:

$$\phi_{i,k}^{n+1} = \phi_{i,k}^n + \Delta t \left(\frac{1}{\rho_i} c_k^n \pm \phi_{i,k}^n \partial_z v_k^n \phi_{i,k}^n \right) \quad (15)$$

$$z_k^{n+1} = z_k^n + \Delta t v_k^n, \quad (16)$$

In order to update the mesh coordinates according to Eq. (16) for the vertical velocity closure derived before, we need to numerically approximate Eq. (7) at each node z_k , which results in

$$320 \quad v(z_k) = \sum_{j=0}^k \left(\frac{1}{\eta} \sigma_j^m \right) \Delta z_j \quad (17)$$

with $\Delta z_j := z_j - z_{j-1}$, $\Delta z_j := z_{j+1} - z_j$ with $j \in [0, nz]$, m Glen exponent, η viscosity and σ_j denoting the stress exerted by the overburdened snow mass

$$\sigma_j = \sum_{l=j}^{nz} g \phi_{i,l} \rho_i \Delta z_l. \quad (18)$$

with g gravitational acceleration. Note, that the stress at the uppermost node $k = nz$ is zero, so that velocity $v(z_{nz})$ is only controlled by the movement below and is thus equivalent to the velocity at the next lower node ($v(z_{nz-1})$). The forward Euler scheme of Eqs. (15) and (16) via the method of characteristics combined with the velocity update (Eq. (17)) essentially resembles the treatment of mass conservation as it is e.g., for instance presently done in SNOWPACK. However, the explicit formulation and numerical treatment of Eqs. (15) and (16) allows to employ also other (e.g. higher order, implicit, etc.) solution schemes for both equations, if this was required to capture detailed aspects of the spatio-temporal coupling of phase changes (c) and settling (via $\partial_z v$) (cf. also the discussion in Sect. 5). To solve Eq. (15), we directly discretize the velocity's spatial derivative $\partial_z v$, which corresponds to the strain rate $\dot{\epsilon}_k^n = \frac{1}{\eta} \sigma_k^m$ given via Eq. (3). This is beneficial, as it avoids ~~to numerically approximate numerically approximating~~ the velocity gradient. The complete numerical update of ice volume fraction ϕ_i and mesh coordinates z can now concisely be written as

$$\phi_{i,k}^{n+1} = \phi_{i,k}^n + \Delta t \left(\frac{1}{\rho_i} c_k^n + \frac{1}{\eta} \left(\sum_{l=j}^{nz} g \phi_{i,l}^n \rho_i c_l \Delta z_l^n \right)^m \phi_{i,k}^n \right) \quad (19)$$

$$335 \quad z_k^{n+1} = z_k^n + \Delta t \left(\sum_{j=0}^k \frac{1}{\eta} \left(\sum_{l=j}^{nz} g \phi_{i,l}^n \rho_i \Delta z_l^n \right)^m \Delta z_j \right). \quad (20)$$

Similar to existing layer-based schemes (see for instance Sect. 3.4. in Bartelt and Lehning (2002) or its recent extension Jafari et al. (2020)), the method of characteristics provides information on the settling of layers within the snowpack. Yet in addition, it serves as a basis for a fully modular and flexible computational strategy, that a) by construction accounts for the two-way feedback between the ice volume fraction and mass production or decay rates resulting from phase changes as a response to transport processes ~~with-in-within~~ the snowpack, b) allows for a flexible adoption/extension of the process model (used to determine c) and the velocity closure. The latter could for instance serve as a pathway to integrate a data-driven velocity closure (or assimilation) from measurements. Such flexibility in numerical tools will be important in the future to conduct model comparisons, such as presented in ~~? Schürholt et al. (20202021)~~ within holistic snowpack models, or even a formalized Bayesian model selection that allows ~~to infer on inferring~~ the most plausible process model out of a pool of candidate models given a certain data. A remaining difficulty now is to provide a (Eulerian) numerical scheme for diffusive processes that can operate on a spatially varying unstructured mesh.

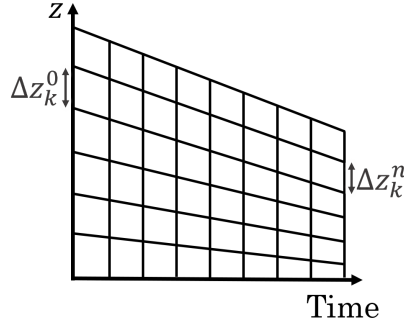


Figure 1. The snowpack height varies with time, e.g. shrinks due to settling of the snow. This has to be incorporated into the computational mesh, which undergoes deformation due to the downward movement of the free surface. The initially equidistant mesh does not uniformly change, which results ~~into~~ in a mesh of varying node distances, so that in general $\Delta z_k^0 \neq \Delta z_k^n$ and $\Delta z_k^n \neq \Delta z_{k+1}^n$.

3.4 Eulerian solution of transport and phase changes on a moving mesh

The process model accounting for ~~heat transport~~ vapor transport and heat transport (Eqs. (9) and ~~vapor transport~~ (11)) has to be solved with respect to a moving computational mesh according to Eq. (16). Both equations have the same generic structure, namely

$$\alpha \partial_{T,t} T - \partial_z (\beta \partial_z T) = \gamma \quad (21)$$

with

$$\begin{aligned} \alpha = \alpha_T = (\rho C)_{eff} + (1 - \phi_i) \frac{d\rho_v^{eq}(T)}{dT} L \quad , \quad \beta = \beta_T = k_{eff} + L D_{eff} \frac{d\rho_v^{eq}(T)}{dT} \quad \text{and} \quad \gamma = \gamma_T = 0 \quad \text{for heat equation Eq. (11), and} \\ \alpha = \alpha_c = (1 - \phi_i) \frac{d\rho_v^{eq}(T)}{dT} \quad , \quad \beta = \beta_c = D_{eff} \frac{d\rho_v^{eq}(T)}{dT} \quad \text{and} \quad \gamma = \gamma_c = -c \quad \text{for vapor transport equation Eq. (9).} \end{aligned} \quad (22)$$

An implicit first order finite difference approximation of Eqs. (9) and (11) for a spatially varying mesh of increments Δz_k^n results in

$$\alpha_{T,k}^n \frac{T_k^{n+1} - T_k^n}{\Delta t} = \frac{2 \cdot (\beta_{T,k+1/2} (T_{k+1}^{n+1} - T_k^{n+1}) - \beta_{T,k-1/2} (T_k^{n+1} - T_{k-1}^{n+1}))}{(\Delta z_k^n)^2 + (\Delta z_{k-1}^n)^2} - E_T(T_{k+1}^n, T_k^n, T_{k-1}^n) \quad (23)$$

$$\alpha_{c,k}^n \frac{T_k^{n+1} - T_k^n}{\Delta t} = \frac{2 \cdot (\beta_{c,k+1/2} (T_{k+1}^{n+1} - T_k^{n+1}) - \beta_{c,k-1/2} (T_k^{n+1} - T_{k-1}^{n+1}))}{(\Delta z_k^n)^2 + (\Delta z_{k-1}^n)^2} - c_k^{n+1} - E_c(T_{k+1}^n, T_k^n, T_{k-1}^n). \quad (24)$$

Note that parameters α_f and β_f for $f \in \{T, c\}$ also vary in space and time, and will be (explicitly) evaluated based on the snowpack's state at time n . $\beta_{f,k\pm 1/2}$ accounts for the parameter's arithmetic mean between two neighboring cells. The terms E_c and E_T are ~~error terms~~ higher-order mesh errors for the vapor and temperature equations, ~~controlled by the temperature gradient. These error terms.~~ These higher-order mesh errors account for the necessary correction due to non-uniformity of

the mesh and are controlled by the temperature gradient; they vanish for equidistant meshes. ~~Their complete form or constant temperatures.~~ The complete form of the higher-order mesh errors is given in Appendix B, and their effect on the accuracy of the simulation is discussed in Sect. 4.3.

365 The complete numerical update can be concisely written in matrix form, which matches with the way it is implemented in the software

$$T^{n+1} = \mathbf{A}_T^{-1} \left(\mathbf{B}_T T^n + \mathbf{E}_T \mathbf{E}_T T^n \right) \quad (25)$$

$$c^{n+1} = \mathbf{A}_c T^{n+1} + \mathbf{B}_c T^n + \mathbf{E}_c \mathbf{E}_c T^n. \quad (26)$$

First, Eq. (25) is solved for temperature T^{n+1} . Next, the updated temperature is used to solve Eq. (26) for the deposition rate c^{n+1} . The complete matrix definitions are given in Appendix C. Note, that formally, it would be possible to add up matrices \mathbf{B}_T and \mathbf{E}_T as well as \mathbf{B}_c and \mathbf{E}_c . We decided to keep them in this particular form to stress the similarity of this formulation with a standard finite difference approximation on an equidistant mesh, in which we are left with \mathbf{B}_T and \mathbf{B}_c and \mathbf{E}_T and \mathbf{E}_c vanish.

3.5 Iterative coupling of Eulerian and Lagrangian solutions

375 The derived numerical update routines for temperature, deposition rate, vertical velocity and ice volume fraction comprise the four main modules that are sequentially called to update the respective state variables for one time step. A schematic illustration is given in Fig. 2. The equations for heat and vapor transport have already been implemented by Calonne et al. (2014) and Hansen and Foslien (2015). A feedback on the ice volume fraction in the absence of a vertical velocity has been investigated in Part 1 of the companion paper (Schürholt et al., 20202021). The modules for vertical velocity and the coupled update of ice
 380 volume fraction and mesh coordinates, through the method of characteristics is novel in our approach. Our implementation is modular in the sense that it allows for a coupling with other process models that comply with a non-uniform mesh. The time step size for the next time step $n + 1$ is dynamically updated according to the in the computational scheme. Since diffusive processes are dominant, we utilize the mesh Fourier number based on the diffusivity $\frac{\beta_T}{\alpha_T}$ of heat of the current time step n

$$385 \Delta t^{n+1} = \min_k \left(\frac{0.5 \alpha_T^n (\Delta z^n)^2}{\beta_T^n} \frac{0.5 \alpha_{T,k}^n (\Delta z_k^n)^2}{\beta_{T,k}^n} \right). \quad (27)$$

Since this choice for the time step computation did not yield instabilities, we excluded the vapor's diffusivity for the time step computation. ~~The final iterative approach can be summarized as: determine time step size Δt according to Eq., update the temperature field based on Eq., compute the deposition rate with the temperature field based on Eq., determine the vertical velocity with Eqs. Note that in response to settling processes, the mesh sizes vary and decrease (cf. Fig. 1), and , and update~~
 390 ~~the ice volume fraction and the mesh coordinates simultaneously based on Eqs. and . While 1.-3. is a re-implementation of an existing approach previously published by (Hansen and Foslien, 2015; Calonne et al., 2014), their coupling to 4. and 5. constitutes the novelties of our work, see also Fig. 2. Note that 4. is computed as part of 5. in the code. Our implementation is~~

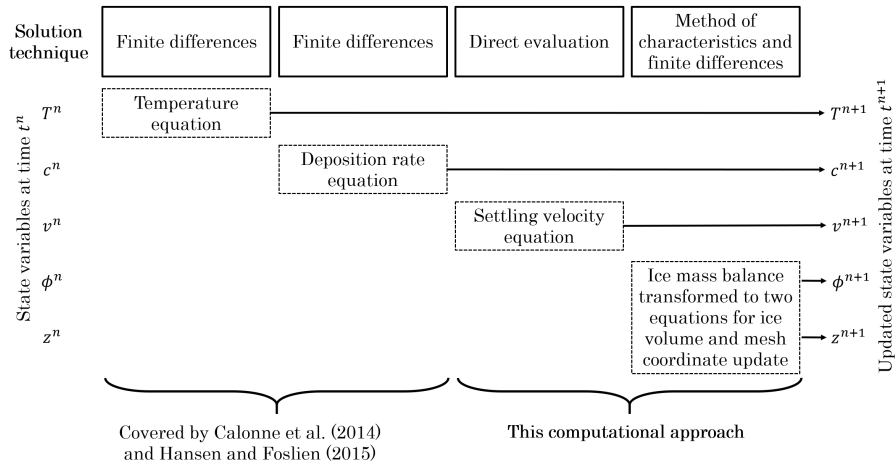


Figure 2. Illustrates the computational workflow of one iteration. The state variables at time t^n , depicted on the left hand side are updated through the modules annotated as dashed boxes ~~and that are~~ ordered diagonally in the centre of the figure. After each update the state variables at time t^{n+1} are retrieved. The equations of the modules are implemented into the computational model through the respective solution technique stated in the solid boxes on the top row. The computational steps are carried out from top to bottom. The ~~equations for heat and vapor transport have already been implemented by Calonne et al. (2014) and Hansen and Foslien (2015)~~ iterative approach can be summarized as: 1) determine time step size Δt according to Eq. A feedback (27), 2) update the temperature field based on Eq. (23), 3) compute the ice volume fraction in deposition rate with the absence of a vertical velocity has been investigated in the companion paper (?) temperature field based on Eq. The modules for (24), 4) determine the vertical velocity with Eqs. (17) and for the coupled (18), and 5) update of the ice volume fraction and the mesh coordinates simultaneously based on Eqs. (19) and (20). While 1)-3) is a re-implementation of an existing approach previously published by Hansen and Foslien (2015); Calonne et al. (2014), through their coupling to 4) and 5) constitutes the ~~method novelties~~ of ~~characteristics~~ our work. Note that 4) is ~~novel~~ computed as part of 5) in ~~our approach~~ the code.

~~modular in the sense that it allows for a coupling with other process models that comply with a non-uniform mesh. so does the time step.~~

395 In the following ~~results (Sect. 4) this modularity is~~, we describe how the modularity of the model is applied and used to assess the individual effect of the different process building blocks by a strategical activation and deactivation of the modules.

3.6 Application of the model

We applied the developed numerical scheme to perform several simulations with varying combinations of *activated* and *de-activated* advection- and diffusion-type process building blocks, e.g. transport and phase changes, such as also considered in
 400 ~~?~~ ~~Schürholt et al. (20202021)~~ vs transport and phase changes in the presence of settling, and their corresponding coupled scenarios. Furthermore, this scheme allowed the numerical verification of separate building blocks. While the scenarios are still idealized, they demonstrate the robustness of the Eulerian-Lagrangian scheme against selection of varying sub-sets of model components. Table 2 provides an overview on the various combinations we considered, as they have been introduced in Sect. 3.

Table 2. List of the various simulation scenarios, referred to as *Cases*, in which we activate different combinations of process building blocks and consider a constant and non-constant viscosity closures. Heat transport induces vapor transport and triggers phase changes. [Case 5](#) and [Case 7 and 8](#) are also referred to as *fully coupled processes*.

Case	Heat Transport (Eq. (23))	Vapor transport (Eq. (24))	Mechanics (Eqs. (19) and (20))			
			Viscosity (Sect. 2.3)		Glen's law (Eq. (17))	
			$\eta = const$	$\eta(\phi_i, T)$	$m = 1$	$m = 3$
Case 1			✓		✓	
Case 2	✓					
Case 3	✓		✓		✓	
Case 4	✓	✓				
Case 5	✓	✓	✓		✓	
Case 6				✓	✓	
Case 7	✓	✓		✓	✓	
Case 8	✓	✓	✓			✓

Note that we used the terms vertical velocity and settling velocity interchangeably.

405 Firstly, we focus on the effects due to pure mechanical settling on the snowpack (Case 1). Next, we consider isolated heat transport (Case 2) as well as its interplay with settling processes (Case 3). Similarly, we consider coupled heat and [water vapor](#) transport first in the absence of settling (Case 4), later with settling (Case 5). For Case 5, we evaluate the effect of included or excluded [error terms higher-order mesh errors](#) E_T and E_c (cf. Sect. 3.4) on the temperature profiles. Case 1, Case 3, and Case 5 consider the constant viscosity for linear Glen's law ($m = 1$) $\eta_{const, m=1}$, as introduced in Sect. 2.3. Furthermore, we
410 investigate the impact of an empirical, temperature and ice volume fraction controlled, viscosity closure (Eq. (4)), first on settling only (Case 6) and then on the fully coupled processes (Case 7). Next, we show that our general approach can be combined with the non-linear Glen's law (Eq. (3)) by using $m = 3$ (Case 8) and an accordingly adjusted constant viscosity $\eta_{const, m=3}$. For a detailed explanation of the general derivation of the viscosity values see Sect. 2.3. Lastly, we compare our new modeling approach to that of a layer-based scheme (Sect. 1).

415 3.7 Computational setup, initial and boundary conditions

Initial condition: The initial ice volume fraction ϕ_i reflects a layered situation as depicted in Fig. 3, with two snow layers of equal thickness. The bottom layer has an initial [effective snow](#) density of 150 kg m^{-3} , and the upper layer's density is 75 kg m^{-3} . The densities are in the range of "damped new snow" and "new snow" respectively (Paterson, 1994). The transition from the upper layer to the lower layer is linearly smoothed out over [over](#) 2 cm, which for a grid defined according to Sect. 3.2
420 corresponds to 5 computational nodes for the coarser and 11 computational nodes for the finer discretization. Temperature is initially constant at a value of 263 K throughout the whole snowpack. Deposition rate is directly deduced from temperature (see 3. in Sect. 3.5) and therefore requires neither initial nor boundary [conditionconditions](#). From the initial condition we derived

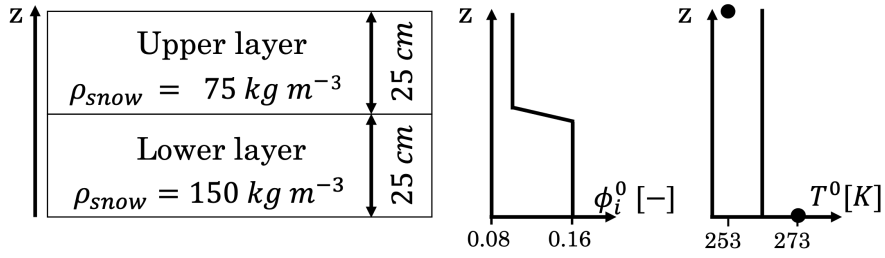


Figure 3. Shows the initial condition of the snowpack regarding snow density at the left hand side and profile plots of the initial ice volume fraction ($\phi_{i,0}$) and temperature (T_0) at the right hand side. There are two snow layers with equal thickness of 25 cm, yielding a snowpack of height 50 cm. The bottom layer has a higher density value of 150 kg m^{-3} and the upper layer's density is 75 kg m^{-3} . The z -axis of the 1d model increases in upward direction, so that $z = 0$ denotes the ground. Downward directed movements are thus described by negative velocities. The interface between the two layers is referred to as transition area. The initial ice volume fraction is derived from initial snow density. Its profile ($\phi_{i,0}$) shows the linear decrease of ice volume fraction in the transition area from the lower to the upper layer. The initial temperature profile (T_0) is constant at 263 K. The black dots mark the constant temperature boundary conditions: 273 K at the bottom; and 253 K at the top.

the constant viscosity values $\eta_{const,m=1} \approx 9.1 \times 10^7 \text{ Pa s}$ and $\eta_{const,m=3} \approx 16 \times 10^{12} \text{ Pa s}$, see also Appendix A3.

Boundary condition: We consider a constant temperature of 273 K at the bottom boundary, and a constant temperature of 253 K at the free surface. **Simulation time:** We simulate 2 days (48 h), 3 days (62 h), and 4 days (96 h) scenarios.

4 Results and Discussion

4.1 Settling (Case 1)

As the first step First, we investigate the effects of mechanical settling on the snowpack (Case 1 in Table 2) and in particular the evolution of the vertical velocity (Fig. 4 (a)) and the ice volume fraction (Fig. 4 (b)). The vertical velocity decreases from top to bottom and relaxes during the first 48 h. ~~Furthermore, the vertical velocity varies less in the upper layer than it does in the lower layer.~~ Vertical velocity varies more in the lower layer. ~~This compared to the upper layer within one time step. This pattern remains prominent as time proceeds, while the overall velocity variation decreases.~~ This effect is due to the increase of the overburdened snow mass from top to bottom. Settling proceeds the fastest just after the start of the simulation, when the snowpack is at maximum height, and correspondingly its ~~effective snow~~ density is the lowest. In the course of time the ice volume fraction increases faster in the lower layer than in the upper layer, and it is the highest at the bottom of the snowpack (Fig. 4 (b)). Furthermore, the extent of the upper layer decreases only slightly ~~with~~, approximately 3.5 cm, over the simulation time, whereas the lower layer reduces to half of its initial height (approximately 12.5 cm). These effects are expected and reflect the correlation between the amount of compaction and the total overburdened mass.

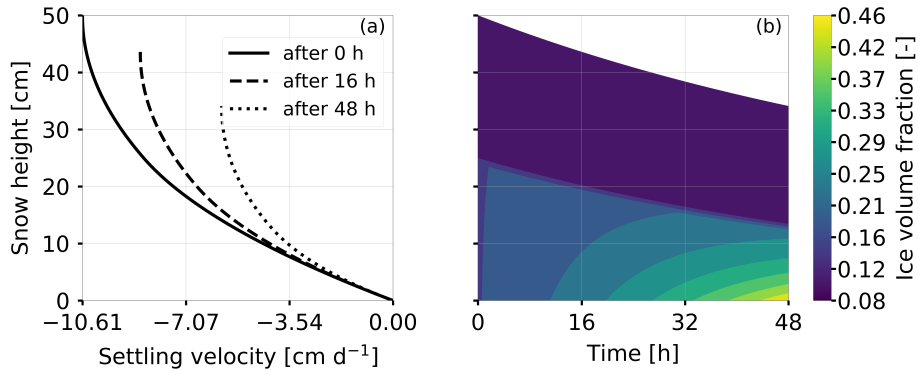


Figure 4. Plots show the results of Case 1 of Table 2, corresponding to isolated settling effects. (a) depicts vertical velocity over snow height. The profiles show the state of the snowpack at initiation, after 16 h and after 48 h. It is clearly visible that vertical velocity and the absolute snow height decrease with time. (b) depicts ice volume fraction over time. ~~Changes~~ We interpret the lower part of the plot, where changes in ice volume fraction are clearly discernible, as the lower layer and the blue area in the upper part of the plot as the upper layer. Changes in ice volume fraction are visible in the lower layer; it increases the most at the bottom of the snowpack.

4.2 Heat transport in the absence and presence of settling (Cases 2 and 3)

440 ~~First, we~~ In this subsection, we first consider isolated heat transport. This simulation scenario refers to Case 2 in Table 2. Temperature (Fig. 5 (a)), and temperature gradients (Fig. 5 (c)) reach a stationary state after approximately 60 h. Heat flux differences between the two layers are clearly visible in the temperature gradient plot. Next, heat transport is superposed by mechanical settling (Fig. 5 (b) and (d)), representing Case 3. As a result, snow height decreases while the internal temperature profiles evolve. Active mechanical processes yield a steepened temperature gradient, hence a higher value of the heat flux
445 (Fig. 5 (d)). This effect can be attributed to:

- the decrease of snow height while keeping the temperatures at the boundaries fixed, and
- the permanent change of thermal conductivity and thermal diffusivity due to their dependency on variations in the ice volume (Eq. (A3)).

The temperature profile will reach the stationary state once the ice volume fraction has reached its maximum value.

450 4.3 Heat and vapor transport in the absence and presence of settling (Cases 4 and 5)

By using the vapor formulation from Hansen and Foslien (2015), transport of vapor through and phase changes in the snowpack both require an apparent temperature gradient, such that the ~~solution evolution~~ of vapor transport ~~should can~~ only be considered in conjunction with heat transport ~~here (Cases 4 and 5 in Table 2)~~. In Fig. 6 (a), we compare the deposition rate (negative for sublimation) due to heat and vapor transport only (Case 4 in Table 2) with the deposition rate obtained when considering
455 additional settling processes, representing the fully coupled processes (Case 5 in Table 2). Both profiles are characterized by

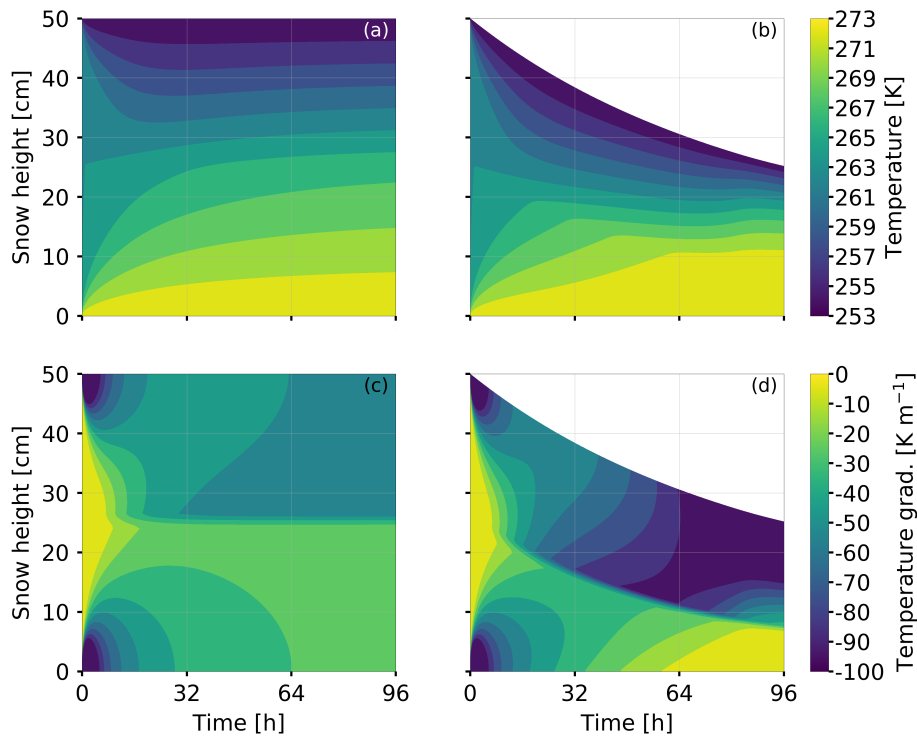


Figure 5. (a) and (c) show the results for Case 2 of Table 2 corresponding to heat transport solely active. (b) and (d) show the results for Case 3 of Table 2 corresponding to active heat transport and mechanical settling. For each plot y-axis represents snow height and x-axis time. The plots in the top row ((a) and (b)) show the temperature evolution, and the plots in the bottom row ((c) and (d)) show the respective temperature gradients. The initial condition for both cases are equivalent (see Fig. 3). In Case 2 the temperature profile (a) has reached the stationary, piecewise linear profile after approximately 60 h. In Case 3 the temperature profile (b) is not yet stationary at the end of the simulation (96 h) as mechanical processes are still yielding a change in ice volume fraction. The temperature gradient (c) will become constant, only when the maximum ice volume fraction has been reached.

moderate deposition rates throughout the snow column with a pronounced negative (sublimation) peak at the centre of the snow column, which is located in the transition area of the layers. ~~This is interpreted as the onset of spatio-temporal oscillations as observed and investigated in greater detail in the companion paper (?). It nicely demonstrates that a) our Eulerian-Lagrangian scheme can capture this behavior, and b) that the instability prevails even in the presence of settling processes. In fact, the~~
 460 ~~The~~ profile for the fully coupled processes shows ~~an even a~~ higher sublimation peak (approximately 4 times). Furthermore, the profiles show a small peak of deposition rate (positive x-direction) just above the aforementioned sublimation rate peak. The latter peak is very weak for Case 4 and more prominent for Case 5. Figure 6 (b) shows the time evolution of the fully coupled processes (Case 5). In the first hours, ~~there is low sublimation taking place~~ sublimation is low in the transition area. After ~~about approximately~~ 6 hours, ~~a the~~ pronounced sublimation rate peak ~~starts to develop that keeps increasing until,~~ as already
 465 described for (a), develops and increases until the end of the simulation (48 h-).

The increased sublimation in the layer transition area may be driven by strong vapor density gradients above the transition area that can be inferred from a strong ~~temperature gradient in that area~~, locally temperature gradient. This temperature ~~variation~~ gradient is further enhanced (Fig. 5 (d)) by compaction due to settling (~~for Case 5, which yields even stronger variations of the material properties in the transition area than without compaction and explains the stronger sublimation rates for the fully~~ coupled processes.

Besides the strong sublimation rate peak also the slight deposition rate peak is highly interesting as it is interpreted as the onset of spatio-temporal oscillations as observed and investigated in greater detail in the companion paper.

(Schürholt et al., 20202021) Schürholt et al. (20202021) describe these wiggles as "smooth oscillations" that are "intrinsic features" of the equations. The results in Fig. 5)6 (a) nicely demonstrate that a) our Eulerian-Lagrangian scheme can capture this behavior, and b) that the instability prevails and even increases in the presence of settling processes. The results suggest that mechanics likely increase local phase change activity in the vicinity of layer boundaries, which potentially has a large effect on weak layer formation.

Lastly, we ~~evaluated the effect of the error terms as introduced in~~ evaluate the impact of included higher-order mesh errors E_T and E_c (cf. Sect. 3.4~~for Case 5. To do so, we derived the weighted mean of the deviations of the temperature distribution~~ obtained without error terms from that with error terms in Eqs. (and)) on the temperature distribution. We determine the error by computing the temperature deviation between the solution that considers higher order mesh errors, and the solution that does not. The deviation is then quantified in an L1 norm. From the temperature error, the deposition error can be derived. The error increases with simulation time and is 0.017 K after 24 h, 0.063 K after 36 h, and 0.183 K after 48 h. After 48 h the deviation is highest for the computational nodes just above the layer transition, where high temperature gradients are present (cf. Fig. 5). Note, that the error for deposition rate could be derived similarly. However, as deposition rate is directly derived from temperature via the vapor transport equation, we consider one error measure as sufficient to emphasize the impact of mesh errors.

4.4 Settling-induced evolution of the ice volume fraction in the absence and presence of transport (Cases 1 and 5)

In this section, we compare isolated settling (Case 1 in Table 2) and the fully coupled processes (Case 5 in Table 2) with respect to their impact on the evolving ice volume fraction. Figure 7 shows the corresponding ice volume fraction profiles after 2 days. Both profiles are very similar (a), which suggests that the density evolution is dominated by settling processes ~~, whereas and~~ coupled heat and vapor transport play a minor role. When focusing on the upper boundary of the transition area (Fig. 7 (b)), we however find a ~~localized locally~~ decreased ice volume fraction for the fully coupled processes (Case 5). This suggests a ~~localized local~~ ice volume decay for active vapor transport and implies phase changes. This observation is consistent with the ~~earlier observed~~ enhanced sublimation rate observed in Fig. 6 indicating the formation of a density heterogeneity.

4.5 Heat and vapor transport coupled to settling with a dynamic viscosity (Case 4, 6, and 7)

Figure 8 (Case 7 in Table 2), finally, shows the evolution of ice volume fraction and viscosity over time for 4 days. Ice volume fraction increases gradually throughout the snow column (Fig. 8 (a)). In Fig. 8 (b), we see that the viscosity of the upper layer

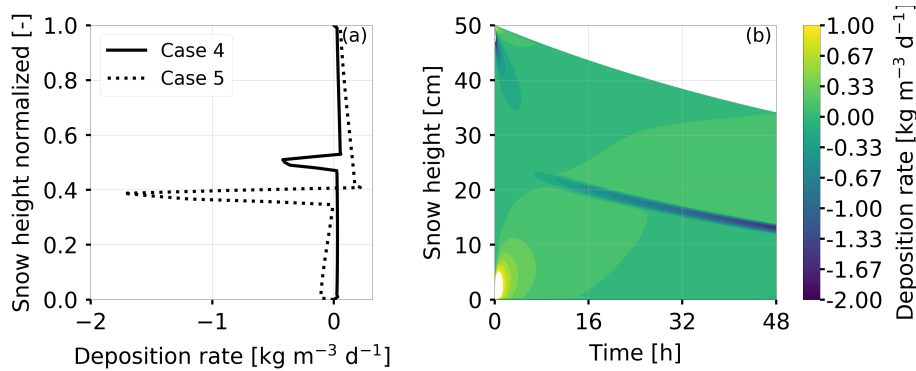


Figure 6. (a) shows two deposition rate profiles over normalized snow height after 2 days. The solid line represents the results of heat and vapor transport in the absence of settling for Case 4 of Table 2. The dashed line refers to Case 5 of Table 2 that additionally accounts for settling. Sublimation rates (negative deposition rates) for Case 5 (fully coupled processes) are increased by approximately a factor of 4 with respect to a Case 4 without settling. At the top of the sublimation peak for both cases, a slight peak in deposition rate is visible. (b) shows the deposition rate profile evolution for Case 5. A pronounced sublimation rate peak in the transition area is first visible after approximately 6 h and increases with time. The lobes at the top and bottom at the start of the simulation are due to the strong phase change activity triggered by the initial and boundary conditions.

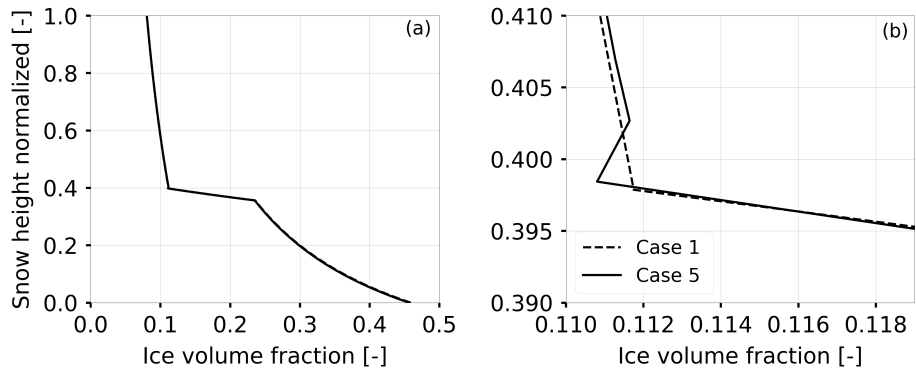


Figure 7. The plots show ice volume fraction profiles over normalized snow height after 2 days. The dashed line (a) depicts ice volume fraction for Case 1 of Table 2 corresponding to solely active settling, whereas and the solid line depicts ice volume fraction computed based on Case 5, which refers to the fully coupled processes. (b) zooms into the density transition area of (a) and shows the effect of the increased sublimation in Fig. 6 on ice volume fraction. In order to better resolve the kink of Case 5, we increased the number of grid nodes to 251.

has smaller values and also increases slower, and they also increase more slowly compared to viscosity values in the lower layer. In contrast, viscosity increases by approximately one magnitude in the lower layer. The This derives from the applied viscosity formula that is controlled by the variables temperature and ice volume fraction. Based on the formula viscosity varies more with respect to ice volume fraction changes than to temperature changes. Ice volume fraction varies more in the lower layer which then also yields more variation in viscosity. Additionally, the height of the lower layer decreases less than the height

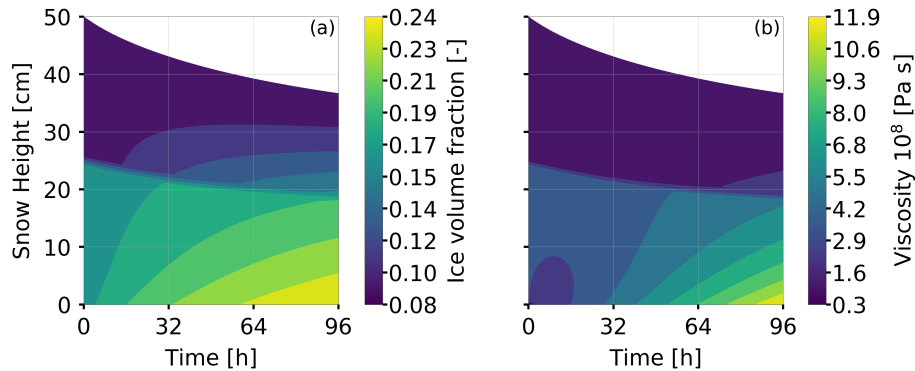


Figure 8. The plots show the evolution of ice volume fraction (a) and viscosity (b) for 4 days for Case 7 of Table 2, which refers to the fully coupled processes combined with dynamically varying viscosity. Snow height is depicted on the y-axis. In (a) ice volume fraction increases most at the bottom of the upper layer. The lower layer consolidates less than the upper layer. In (b) viscosity increases slower in the upper layer and increases faster (up to one magnitude) in the lower layer.

that of the upper layer. This outcome may be related to the lower layer's higher viscosity (higher resistance to deformation).

505 Figure 9 (a) compares the ice volume fraction profiles after three days simulation time of Case 7 to that of Case 6 (fully coupled processes, non-dynamic viscosity). For the dynamic viscosity, ice volume fraction is higher in the lower layer and lower in the upper layer compared to that of constant viscosity. This is due to the dynamic viscosity's temperature dependence. Temperatures at the bottom are close to the melting point and yield lower viscosities. Thus, settling proceeds faster and compaction is stronger in the lower part. The opposite is true for the upper variations. Since we used an intermediate value of

510 263 K to derive the constant viscosity, variations in the centre of the snowpack are less pronounced. Figure 9 (b) shows the deposition rate of Case 7 compared with Case 4, which refers to deactivated settling. Similar as Fig. 6 both deposition rate profiles have a sublimation rate peak in the transition area, and the peak of the fully coupled processes is higher than the one with deactivated settling. Additionally, Case 7 shows the small peak in deposition rate just above the sublimation rate peak as explained in Sec. 4.3. Although the simulation time for Fig. 9 (b) was three days, the sublimation rate peak of Case 7 is lower

515 as the one of Case 4 (Fig. 6 (a)) after two days. This suggests that the sublimation rate peak is less pronounced when coupled to the proposed dynamic viscosity.

4.6 ~~Linear versus non-linear~~ Non-linear Glen's law in a fully coupled dry snowpack model of constant viscosity (Cases ~~Case 5 and 8~~)

520 In the final simulation scenario, we ~~compare present the~~ results of the fully coupled processes for ~~different parameters in~~ non-linear Glen's law (Eq. 3), namely $m=1$ in Case 5 and $m=3$ in Case with $m=3$, Case 8). As discussed before (Sect. 2.3), the viscosity closure (whether it is a constant value or an empirical closure) strongly depends on the choice of the Glen parameter m . This requires us to adjust the constant viscosity value accordingly, see Sect. 2.3 for details.

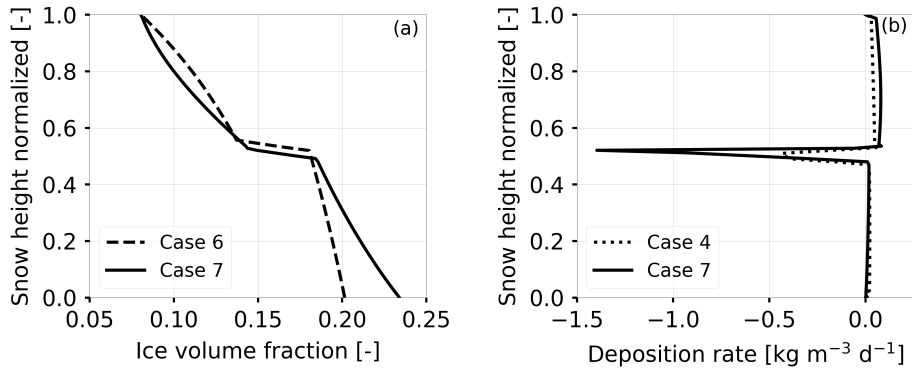


Figure 9. (a) shows ice volume fraction profiles after 3 days simulation time obtained with a dynamic viscosity. Y-axis depicts normalized snow height. The dashed line refers to Case 6 of Table 2 corresponding to mechanical settling solely, and the solid line refers to Case 7, which represents the fully coupled processes. (b) shows deposition rate profiles for Case 7 and Case 4 after 3 days simulation time. Y-axis depicts normalized snow height. The solid line ~~refer~~ refers to Case 7, and the dashed line represents heat and vapor transport in the absence of settling (Case 4). For the fully coupled processes sublimation rate at the layer transition is approximately three times stronger compared with inactive settling (Case 4).

Figure 10 (a) ([Case 8 in Table 2](#)) shows vertical velocity profiles and the evolution of ice volume fraction with time. The vertical velocity is almost constant in the upper layer and then decreases in the lower layer. This effect is similar to the vertical velocity profiles as presented and explained ~~in Sect. 4.1~~ for the linear version of Glen's law ([Fig. 4 \(a\)](#)), but it is more pronounced due to the non-linearity in the constitutive law. Compared with previous scenarios, the overall vertical velocity is lower. This is probably related to the magnitude of the constant viscosity and cannot be directly related to the non-linear constitutive law. A further sensitivity study in the future would be most informative.

In Fig. 10 (b) the upper layer's ice volume fraction and thickness remains almost constant with time. In contrast, the lower layer decreases [9 cm](#) in height, while the ice volume fraction increases with time from top to bottom.

Again, the corresponding deposition rate profile shows a sublimation peak in the layer transition area ([Appendix D1](#)) that increases with time. Overall however, deposition rates tend to be lower compared to preceding computations. The reduced phase change activity in the layer transition area can directly be related to smaller vertical variations in the temperature profile. This effect may be due to less variation in the vertical velocities that yield a more uniform deformation and a less pronounced variation of ice volume fraction across the layer transition area.

4.7 Comparison against layer-based schemes (based on Case 6)

In this section, we compare results of our proposed Eulerian-Lagrangian scheme with conventional layer-based models. We would like to emphasize that a two layer snowpack model certainly constitutes an extremely simplified case, as layer-based schemes are usually operated with a significantly higher number of snow layers. It is yet informative to conduct this analysis to point out ~~this~~ differences, as these can certainly accumulate during long simulation times.

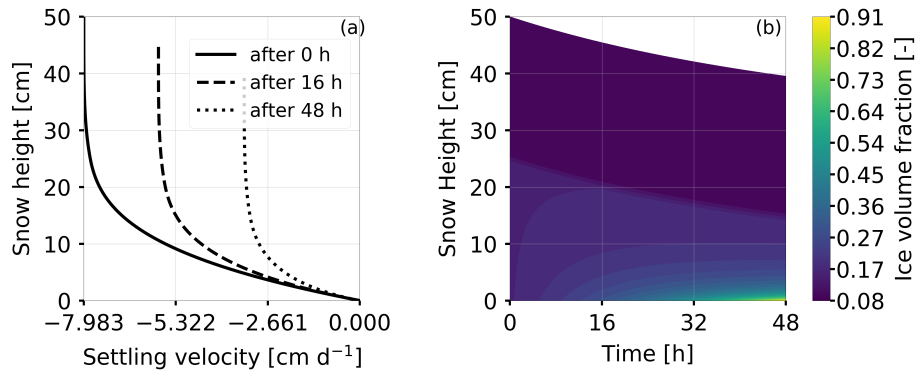


Figure 10. The plots show vertical velocity profiles (a) and ice volume fraction (b) for Case 8 of Table 2, which refers to the fully coupled processes combined with a non-linear Glen's law. Velocity (a) varies less, which yields a more uniform evolution of the snowpack (b).

In layer-based snowpack models state variables are assigned layerwise, and the two layer snowpack (Fig. 3) would have three computational nodes at the following locations: at the bottom of Layer 1-the lower layer, at the top of Layer 1-the lower layer and at the top of Layer 2-the upper layer. The two nodes located at the top of the layers would then represent the physical state of Layer 1 and Layer 2-the lower and the upper layer, respectively. Velocity is again derived from stress exerted by the overburden snow mass. Since Layer 2-the upper layer is represented by the computational node at the top, it is unloaded and requires a special treatment for stress. We adopt the approach by Vionnet et al. (2012) and apply a 'non-physical stress' equivalent to half of the layer's own weight, yet apply it to the uppermost computational node (Sect. 3.4 in Vionnet et al. (2012)). Next, vertical velocity is computed likewise with Eq. (7) and viscosity with Eq. (4). We compare both approaches based on Case 6 of Table 2, hence in the presence of mechanical settling and for a dynamic viscosity closure. Since we neglect heat and vapor transport, the viscosity changes over time are solely due to the evolution of ice volume fraction alone.

In Fig. 11, we see that the layer-based scheme sustains a layer-based vertical velocity (a) and ice volume fraction evolution (c): One value for the velocity and one value for the ice volume fraction describe an entire layer. In contrast, using the generalized Lagrangian approach described in Sect. 3, we yield a sublayer resolution of the vertical velocities (b) and ice volume fractions (d). For both approaches (layer-based and Eulerian-Lagrangian) the vertical velocity is higher in the top part of the snowpack and zero at the bottom. For early times, the layer-based scheme determines a vertical velocity that is one order of magnitude higher than values computed with the Eulerian-Lagrangian scheme. This may be related to the comparably high (non-physical) stress at the top of Layer 2-the upper layer. At the end of the simulation, the snowpack has settled almost twice as much with the layer-based scheme, which highlights the impact of this conceptual difference. This effect may result from an overestimation of velocity with layer-based schemes. Following our proposed method, ice volume fraction is higher in the lower part of the snowpack and reaches higher values (Fig. 11 (d)). Furthermore, ice volume fraction at the top of the snowpack does not change during the simulation since there is no stress from overburden mass. In contrast, for the layer-based scheme ice volume fraction grows at this location (Fig. 11 (c)). This is again due to the chosen stress condition at the top. Of course this discrepancy gets smaller as we increase the number of layers and this effect may reduce. However this slight offset in the stress condition will

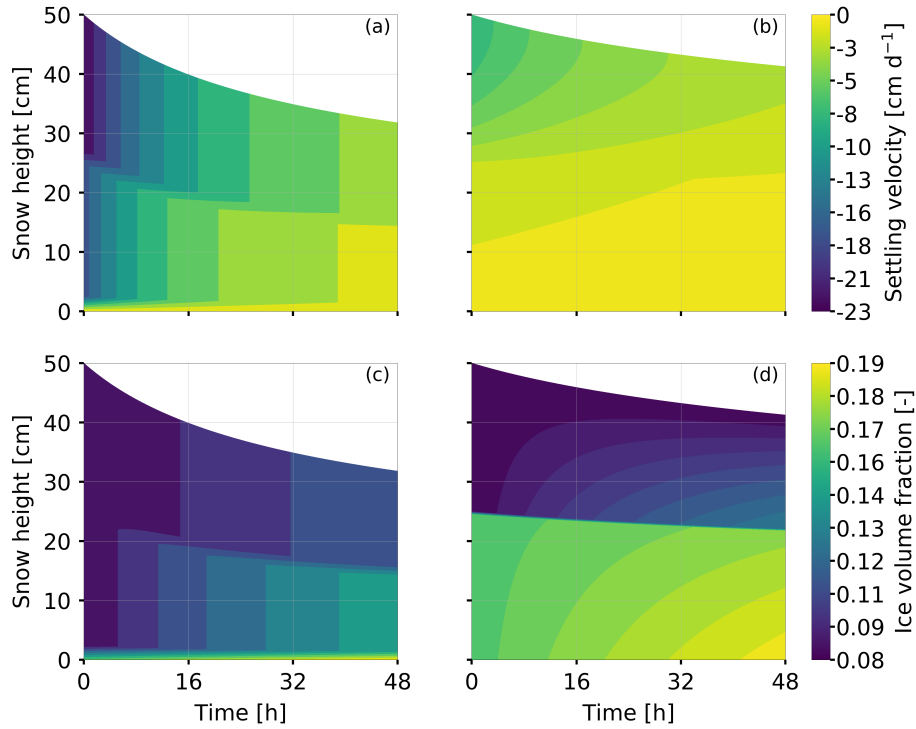


Figure 11. The plots show the temporal evolution of vertical velocity (top row) and ice volume fraction (bottom row) for Case 6 of Table 2 corresponding to solely active mechanical settling. For (b) and (d), we applied our highly discretized settling scheme, and for (a) and (c), we mimicked the layer-wise discretization of layer-based schemes. Y-axis depicts snow height. Snow viscosity is controlled by ice volume fraction alone, since heat transport is inactive. In (a) and (c) Layer 1-the lower and Layer 2-upper layer are resolved. Their respective values refer to the computational nodes at the top and between the two layers. The values retrieved for the lowest node, do not represent an entire layer and are depicted at height zero. For the layer-based scheme, one velocity or ice volume fraction value represents the movement or density of the entire layer. In contrast, with our approach vertical velocity varies throughout each layer (b) so that ice volume fraction increases layer internally and develops a gradual pattern (d).

565 always be present and lead to uncertainties. In the proposed computational approach the spatial resolution of processes can be easily changed to assess its impact on snowpack evolution. In a future study, it might be interesting to quantitatively compare results against Jafari et al. (2020), who also rely on a rather fine spatial resolution.

5 Summary and conclusions

In this [article paper](#), we described in detail a hybrid Eulerian-Lagrangian computational approach to model the evolution of a dry snowpack. The model accounts for transport of heat and vapor, phase changes (sublimation and deposition), and mechanical settling processes. The ice mass balance is explicitly accounted for in the model formulation. It captures the evolution of the ice volume fraction in response to settling and phase changes. It constitutes an advection-dominated partial differential

equation of hyperbolic type, and is therefore conveniently solved with the method of characteristics, a popular Lagrangian type scheme for such processes. Here, Lagrangian refers to the fact that the scheme tracks the motion of a snow material "particles" within the snow column by adjusting the node positions, while at the same time it accounts for phase changes within the moving particle. Solving the ice mass balance requires us to specify the vertical velocity as well as the mass production rate (sublimation rate/deposition rate). A closure for the velocity is derived by combining a common mechanical stress-strain relation with Glen's law, and numerically approximating the resulting integrals. The deposition rate is due to vapor transport through a varying temperature field, and can be determined from a diffusive type process model that accounts for simultaneous heat and vapor transport. Due to its diffusive type (parabolic), a fixed-grid approach is most appropriate, referred to as an Eulerian approach. More specifically, we solved coupled heat and vapor transport by means of a first order implicit in time finite difference approximation. The Eulerian scheme for the process model's diffusive part complies with the non-uniform mesh that results from the Lagrangian scheme for the ice volume fraction evolution. In order to solve the complete dry snow process model for the coupled evolution of the ice volume fraction, temperature field, vapor field and settling processes, the Eulerian and Lagrangian parts are iteratively applied following a straight-forward operator split approach.

We have implemented our proposed numerical scheme as a series of sequential updates within one simulation time step. The implementation follows a modular, extendable approach, such that each process building block can easily be considered or neglected for verification or validation purposes. We applied our numerical core to conduct a series of simulation scenarios comprising isolated processes (pure settling, pure heat transport), two-process coupling scenarios (heat transport in the presence of settling, coupled heat and vapor transport) and the fully coupled processes (heat and vapor transport in the presence of settling). We furthermore investigated different viscosity closures as well as a linear and a non-linear version of Glen's law. A two-layer snowpack, consisting of a lower layer of higher density and an upper layer of lower density, served as a test case to demonstrate the feasibility of our approach. We simulated fields and profiles for temperature, deposition rate, ice volume fraction and vertical velocity with a high spatial (~mm to cm) and temporal (~min) resolution.

We found that

- Our Eulerian-Lagrangian scheme along with its vectorized implementation is flexible and extendable. Alternative model closures, e.g. for the viscosity and the vertical velocity can easily be integrated. To close for the velocity, we have successfully tested a non-linear strain rate closure commonly used in firn models (Lundin et al., 2017). The Lagrangian part of the solver (that accounts for the evolution of the ice volume fraction) could easily be singled out and coupled to an alternative process model, e.g. when accounting for firn conditions instead of dry snow.
- Although within this paper, we mostly relied on numerical approximations that are of either first order (time integration/operator splitting) or second order (diffusion operator), the corresponding numerical solvers can be extended without a conceptual difficulty, e.g. changing from a first order time integration to an higher order in time integrator. We commented on this in the respective section [\(Sec. 3\)](#).

- 605 – The combination of an implicit Eulerian routine for the diffusion-dominated operators (that controls the time stepping) and a Lagrangian routine for the advection-dominated operators ran stable and robust for all considered simulation cases (different viscosity closures, different versions of Glen’s law).
- The numerical scheme allows for a high spatial resolution that resolves processes on the sublayer level. By construction, it relies on a mechanically consistent vertical velocity. This improves the accuracy since it makes the ad-hoc specifica-
610 tion of an artificial stress value for the uppermost layer ~~Vionnet et al. (2012)~~ (e.g. [Vionnet et al. \(2012\)](#)), as required for conventional layer-based schemes, obsolete.
- The modular setup of the software facilitated a systematic study of various models formulations, in which we selectively considered different combinations of process building blocks without fine-tuning the stability of the solver. This is important to enable empirical-numerical investigations of the relevance of different process couplings (see next point).
- 615 – Our simulation consistently showed that vapor transport and phase change in the presence of strong temperature gradients can induce a stronger phase change activity, and in particular a localized sublimation rate peak above the transition area between two layers. We furthermore showed that this has the potential to result into a localized ice volume fraction reduction above the transition area. This in itself is not new, as a similar behavior has been deduced in Hansen and Foslien (2015) and analyzed in detail in our companion paper ~~?~~ [Schürholt et al. \(20202021\)](#). In addition to the existing
620 results, however, we have shown that the increased phase change activity persists in the presence of settling (even more pronounced), for both a constant and a dynamic viscosity closure, and for a linear as well as a non-linear version of Glen’s law.
- The incorporation of the ~~Error terms~~ [higher-order mesh errors](#) in the vapor and heat transport equations that account for deviations due to the non-uniform mesh increases accuracy especially in areas with large node distances and high
625 temperature gradients.

In our [article paper](#), we deliberately focused on discussing modularity and extendability in the context of snowpack modeling, e.g. by assessing a whole process cascade for one relatively simplified physical setting. In order to discuss these aspects in-depth, we restricted ourselves to one relatively simply physical setting. We are well aware that as of today, our proposed numerical approach is not ready for operational use, and that was not our intention. At this point in time, we rather would
630 like to contribute to the discussion how future snowpack modeling can benefit from a consistently formulated, hybrid Eulerian Lagrangian solver. Nevertheless, it is important to discuss, whether the suggested scheme is amenable to further extensions required for an operational snowpack model.

Most importantly, the proposed scheme would need a generalization for surface mass gain (precipitation) or losses (sublimation). This bears two technical challenges. First, concurrent settling and precipitation result in a non-monotonic vertical
635 motion of the snowpack’s upper surface, for which several techniques have been proposed in the past, e.g. based on a regularization approach (Wingham, 2000) or via a kinetic boundary conditions as applied for sedimentation on ocean floors in ~~(Audet and Fowler, 1992)~~ [Audet and Fowler \(1992\)](#). A straight-forward approach based on appending the computational grid

sequentially during precipitation events likewise seems computationally feasible. A second challenge associated with the incorporation of precipitation events is the question of how to initialize the complete state (temperature, vapor and deposition rate) in the new snow layers. The latter is less critical in conventional layer-based schemes, as the necessary information reduces to 'one value per layer'. While the first challenge mostly means to overcome technical subtleties in the actual implementation, the second requires a thoughtful formulation of physically consistent boundary conditions. Neither of the two challenges seem to pose a severe risk.

Another important addition to our proposed snowpack model is the presence of liquid water in the snow. ~~While its pure~~ Conceptually, similar modeling approaches could be used to derive a model for wet snow. While including potential phase changes from melting/freezing could be straight-forwardly implemented via the source term c , it is the advective transport of liquid water that is more demanding. Liquid water transport is commonly modeled via the Richards equation (Wever et al., 2014) which would benefit from existing hybrid Eulerian-Lagrangian solution strategies, as shown for saturated media without mechanical settling (Huang et al., 1994). Furthermore, a model for wet snow requires a second energy balance to account for the liquid water temperature. Once set up, it can be integrated into our computational workflow (Fig. 2).

Finally, operational models generally include the capability to account for topological change within the snow column, to capture layer coalescence if two initially separated snow layers merge into one, or layer separation, if an initially homogeneous layer splits into two. By construction, our computational approach does not require a dedicated treatment for layer coalescence or separation. Both are implicitly accounted in the continuous description of stratigraphy as long as the feature that is to be resolved is larger than the chosen spatial resolution of the computational grid. Otherwise the resolution can be increased to avoid layer split ups for regions with high gradients. Furthermore, our approach prevents the complete degeneration of layers as the ice volume fraction is constrained by the snow's maximum apparent density per construction of the scheme. Yet, while the theory suggests that layer coalescence and separation are not problematic, their might still be troublesome realistic test cases, especially when thinking about long simulation times. In order to address these and verify robustness, a series of benchmark tests have to be conducted. If necessary, the Lagrangian-Eulerian scheme in its current version can be equipped with occasional re-meshing (along with a re-sampling of field variables) triggered by the degeneration of well defined mesh quality criteria.

We believe that a flexible and extendable computational approach, such as the one described in this articlepaper, will be key for future snowpack modeling, to facilitate the use of standardized benchmark problems (potentially used during a continuous integration) and allow us to systematically assess the model's predictive power, including uncertainty quantification, parameter estimation and model selection.

Code availability. The code will be made available upon acceptance.

Appendix A: Formulas required for the process model

A1 Vapor saturation density

An empirical expression for the vapor saturation density $\rho_v^{eq}(T)$ in terms of temperature T is formulated based on the empirical
670 formulation for vapor saturation pressure from Libbrecht (1999) and reads

$$\rho_v^{eq}(T) = \frac{\exp(-\frac{T_{ref}}{T})}{fT} (a_0 + a_1(T - 273T_m) + a_2(T - 273T - T_m)^2) \quad (A1)$$

with coefficients $a_0 = 3.6636 \times 10^{12} \text{ kgm}^{-1}\text{s}^{-2}$, $a_1 = -1.3086 \times 10^8 \text{ kgm}^{-1}\text{s}^{-2}\text{K}^{-1}$, $a_2 = -3.3793 \times 10^6 \text{ kgm}^{-1}\text{s}^{-2}\text{K}^{-2}$,
675 $f = 461.31 \text{ as well as reference temperature-J kg}^{-1}\text{K}^{-1}$, $T_m = 273.15 \text{ K}$ $T_{ref} = 6150 \text{ K}$. Note that fT accounts f is the
specific gas constant for water vapor. Note that division by fT account for the conversion from pressure Pa to with the ideal
gas law (as used in Part 1) to density kgm^{-3} .

A2 Model parameters in the transport and phase change equations

The effective vapor mass diffusion coefficient $D_{eff}(\phi_i)$ in terms of ice volume fraction ϕ_i is taken from Calonne et al. (2011),
but is extended by the heaviside function $HS\Theta$ to hinder vapor diffusion for ice volumes above $\frac{2}{3}$

$$D_{eff}(\phi_i) = D_0(1 - \frac{3}{2}\phi_i) HS\Theta\left(\frac{2}{3} - \phi_i\right), \quad (A2)$$

680 with $D_0 = 2.036 \times 10^{-5} \text{ m}^2\text{s}^{-1}$ the vapor diffusion constant in air.

The effective thermal conductivity $k_{eff}(\phi_i)$ in terms of ice volume fraction ϕ_i is taken from Calonne et al. (2011) and reads

$$k_{eff}(\phi_i) = a_0 + a_1(\phi_i \rho_i) + a_2(\rho_i \phi_i)^2 \quad (A3)$$

with coefficients $a_0 = 0.024$, $a_1 = -1.23 \times 10^{-4}$ and $a_2 = 2.5 \times 10^{-6}$ and ice density ρ_i .

The effective heat capacity $(\rho C)_{eff}(\phi_i)$ in terms of ice volume fraction ϕ_i is taken from Calonne et al. (2014) and Hansen and
685 Foslien (2015) and reads

$$(\rho C)_{eff}(\phi_i) = \phi_i \rho_i C_i + (1 - \phi_i) \rho_a C_a, \quad (A4)$$

with C_i ice heat capacity, C_a air heat capacity and ρ_i ice density and ρ_a air density.

A3 Constant viscosity for the two layer case

A3.1 Linear Glen's law, $\eta_{const,m=1}$

690 We derived intermediate ice volume fraction $\phi_{i,const} = 0.1125$ and temperature $T_{const} = 263 \text{ K}$ values from the initial condi-
tion of the two layer case and insert them as constants into Eq. (4).

A3.2 Non-linear Glen's law $\eta_{const,m=3}$

Equation (4) does not hold for Glen exponent $m = 3$, therefore we derive an adjusted constant viscosity $\eta_{const,m=3}$ via the constitutive equation (Eq. (3))

$$695 \quad \dot{\epsilon}_{lit} = \frac{1}{\eta_{const,m=3}} \sigma_{max}^m, \quad (A5)$$

with $\dot{\epsilon}_{lit} \equiv 10^{-6} \text{ s}^{-1}$ a strain rate value from the literature Johnson (2011) and $\sigma_{max} \equiv 547.71 \text{ Pa}$ the maximum stress value obtained from the initial snow density profile of the two layer case. Eq. (A5) is then solved for the constant viscosity $\eta_{const,m=3}$.

A3.3 Restrict infinite ice volume growth

To hinder infinite ice volume growth, the constant viscosity $\eta_{const,m}$ is combined with a power law that yields exponential
700 growth of viscosity for cells with $\phi_i > 0.95$

$$PL(\phi_i) = \exp(pl1 \phi_i - pl2) + 1, \quad (A6)$$

with ~~$pl1 = 690$~~ $pl1 = 690$ and $pl2 = 650$. The constant viscosity is then multiplied with the power law ($\eta_{const,m} PL(\phi_i)$), so that computational nodes with $\phi_i > 0.95$ are assigned and viscosity grows exponentially. Note that for better readability the multiplication with the power law is omitted in the equations of this paper.

705 Appendix B: ~~Mesh error terms due~~ Higher-order mesh errors to correct for non-uniform mesh

For the temperature equation Eq. (23) the higher-order mesh error is

$$E_T(T_{k+1}^n, T_k^n, T_{k-1}^n) = \frac{\Delta z_k^n - \Delta z_{k-1}^n}{\Delta z_k^n + \Delta z_{k-1}^n} \frac{2 \cdot (\beta_T (T_{k+1}^{n+1} - T_k^{n+1}) - \beta_T (T_k^{n+1} - T_{k-1}^{n+1}))}{(\Delta z_k^n)^2 + (\Delta z_{k-1}^n)^2}, \quad (B1)$$

and for the vapor transport equation Eq. (24) it is

$$E_c(T_{k+1}^n, T_k^n, T_{k-1}^n) = \frac{\Delta z_k^n - \Delta z_{k-1}^n}{\Delta z_k^n + \Delta z_{k-1}^n} \frac{2 \cdot (\beta_c (T_{k+1}^{n+1} - T_k^{n+1}) - \beta_c (T_k^{n+1} - T_{k-1}^{n+1}))}{(\Delta z_k^n)^2 + (\Delta z_{k-1}^n)^2}. \quad (B2)$$

710 For the matrix equations Eqs. (26) and (25) the higher-order mesh errors are defined as \mathbf{E}_T and \mathbf{E}_C .

Appendix C: Matrices from temperature and vapor transport equations

Matrix **A** is defined as follows:

$$\mathbf{A} = \begin{pmatrix} A_{m,0}^n & 0 & 0 & \cdots & 0 & 0 & 0 \\ A_{l,1}^n & A_{m,1}^n & A_{u,1}^n & \cdots & 0 & 0 & 0 \\ 0 & A_{l,2}^n & A_{m,2}^n & \cdots & 0 & 0 & 0 \\ \vdots & \vdots & \vdots & \ddots & \vdots & \vdots & \vdots \\ 0 & 0 & 0 & \cdots & A_{m,nz-2}^n & A_{u,nz-2}^n & 0 \\ 0 & 0 & 0 & \cdots & A_{l,nz-1}^n & A_{m,nz-1}^n & A_{u,nz-1}^n \\ 0 & 0 & 0 & \cdots & 0 & 0 & A_{m,nz}^n \end{pmatrix} \quad (\text{C1})$$

For the heat equation (Eq. (25)) (\mathbf{A}_T) the entries are

$$715 \quad A_{l,k}^n = -D_k^n (\beta_{T,k}^n + \beta_{T,k-1}^n) \quad (\text{C2})$$

$$A_{u,k}^n = -D_k^n (\beta_{T,k+1}^n + \beta_{T,k}^n) \quad (\text{C3})$$

$$A_{m,k}^n = \alpha_{T,k}^n + D_k^n (\beta_{T,k+1}^n + 2\beta_{T,k}^n + \beta_{T,k-1}^n) \text{ with } A_{m,0}^n = 1 \text{ and } A_{m,nz}^n = 1 \quad (\text{C4})$$

with

$$D_k^n = \frac{\Delta t^n}{(\Delta z_k^n)^2 + (\Delta z_{k-1}^n)^2}. \quad (\text{C5})$$

720 For the vapor transport (Eq. (26)) (\mathbf{A}_c) the entries are

$$A_{l,k}^n = \frac{1}{(\Delta z_k^n)^2 + (\Delta z_{k-1}^n)^2} (\beta_{c,k}^n + \beta_{c,k-1}^n) \quad (\text{C6})$$

$$A_{u,k}^n = \frac{1}{(\Delta z_k^n)^2 + (\Delta z_{k-1}^n)^2} (\beta_{c,k}^n + \beta_{c,k+1}^n) \quad (\text{C7})$$

$$A_{m,k}^n = \frac{\alpha_{c,k}^n}{\Delta t^n} + \frac{1}{(\Delta z_k^n)^2 + (\Delta z_{k-1}^n)^2} (\beta_{c,k-1}^n + 2\beta_{c,k}^n + \beta_{c,k+1}^n) \text{ with } A_{m,0}^n = -\frac{\alpha_{c,0}^n}{\Delta t^n} \text{ and } A_{m,nz}^n = -\frac{\alpha_{c,nz}^n}{\Delta t^n}. \quad (\text{C8})$$

Matrix **B** is defined as follows:

$$725 \quad \mathbf{B} = \begin{pmatrix} \alpha_{m,0}^n & 0 & 0 & \cdots & 0 & 0 & 0 \\ 0 & \alpha_{m,1}^n & 0 & \cdots & 0 & 0 & 0 \\ 0 & 0 & \alpha_{m,2}^n & \cdots & 0 & 0 & 0 \\ \vdots & \vdots & \vdots & \ddots & \vdots & \vdots & \vdots \\ 0 & 0 & 0 & \cdots & \alpha_{m,nz-2}^n & 0 & 0 \\ 0 & 0 & 0 & \cdots & 0 & \alpha_{m,nz-1}^n & 0 \\ 0 & 0 & 0 & \cdots & 0 & 0 & \alpha_{m,nz}^n \end{pmatrix} \quad (\text{C9})$$

For Eq. (25) (\mathbf{B}_T) the entries are

$$\alpha_{m,k}^n = \alpha_{T,k}^n \quad (\text{C10})$$

and for Eq. (26) (\mathbf{B}_c)

$$\alpha_{m,k}^n = \alpha_{c,k}^n \frac{\alpha_{c,k}^n}{\Delta t^n}. \quad (\text{C11})$$

730 Matrix \mathbf{E} is defined as follows

$$\mathbf{E} = \begin{pmatrix} 0 & 0 & 0 & \cdots & 0 & 0 & 0 \\ E_{l,0}^n & E_{m,1}^n & E_{u,1}^n & \cdots & 0 & 0 & 0 \\ 0 & E_{l,1}^n & E_{m,2}^n & \cdots & 0 & 0 & 0 \\ \vdots & \vdots & \vdots & \ddots & \vdots & \vdots & \vdots \\ 0 & 0 & 0 & \cdots & E_{m,nz-2}^n & E_{u,nz-2}^n & 0 \\ 0 & 0 & 0 & \cdots & E_{l,nz-1}^n & E_{m,nz-1}^n & E_{u,nz-1}^n \\ 0 & 0 & 0 & \cdots & 0 & 0 & 0 \end{pmatrix}, \quad (\text{C12})$$

consisting of the following terms

$$E_{m,k}^n = f_{\Delta z,k}^n \beta_{r,k}^n - f_{\Delta z,k}^n \beta_{l,k}^n \quad (\text{C13})$$

$$E_{l,k}^n = -f_{\Delta z,k}^n \beta_{r,k}^n \quad (\text{C14})$$

$$735 \quad E_{u,k}^n = f_{\Delta z,k}^n \beta_{l,k}^n, \quad (\text{C15})$$

with

$$\beta_{l,k}^n = 0.5 (\beta_{k+1}^n + \beta_k^n) \quad (\text{C16})$$

$$\beta_{r,k}^n = 0.5 (\beta_k^n + \beta_{k-1}^n) \quad (\text{C17})$$

$$f_{\Delta z,k}^n = \frac{\Delta z_k^n - \Delta z_{k-1}^n}{\Delta z_k^n + \Delta z_{k-1}^n} \frac{1}{(\Delta z_k^n)^2 + (\Delta z_{k-1}^n)^2}. \quad (\text{C18})$$

740 Note that $\beta = \beta_c$ for Eq. (26) and $\beta = \beta_T$ for Eq. (25), as explained in Sect. 3.4

Appendix D: Additional figures

D1 Non-linear Glen's law

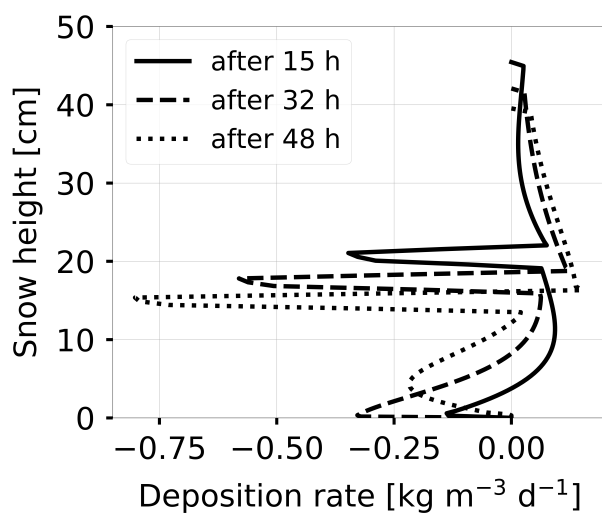


Figure D1. The plot shows the deposition rate profiles for 0, 1.5 and 2 days simulation time for Case 8 (Table 2), which is the fully coupled processes combined with the non-linear Glen's law. Y-axis depicts snow height.

Author contributions. Study concept, underlying model and methodology devised by AS, HL, and JK. Model analysis, software implementation, simulation runs performed by AS supervised by JK. Test case analysis and discussion, data visualization and manuscript preparation
745 was carried out by AS with contributions from JK and HL.

Competing interests. No competing interests are present.

Acknowledgements. The authors were supported by the Helmholtz Graduate School for Data Science in Life, Earth and Energy (HDS-LEE). The work was furthermore supported by the Federal Ministry of Economic Affairs and Energy, on the basis of a decision by the German Bundestag (50 NA 1908).

750 **References**

- Audet, D. and Fowler, A.: A mathematical model for compaction in sedimentary basins, *Geophysical Journal International*, 110, 577–590, <https://doi.org/10.1111/j.1365-246x.1992.tb02093.x>, 1992.
- Bader, H.-P. and Weilenmann, P.: Modeling temperature distribution, energy and mass flow in a (phase-changing) snowpack. I. Model and case studies, *Cold Regions Science and Technology*, 20, 157–181, [https://doi.org/10.1016/0165-232x\(92\)90015-m](https://doi.org/10.1016/0165-232x(92)90015-m), 1992.
- 755 Bartelt, P. and Lehning, M.: A physical SNOWPACK model for the Swiss avalanche warning: Part I: numerical model, *Cold Regions Science and Technology*, 35, 123–145, [https://doi.org/10.1016/s0165-232x\(02\)00074-5](https://doi.org/10.1016/s0165-232x(02)00074-5), 2002.
- Brun, E., Martin, E., Simon, V., Gendre, C., and Coleou, C.: An Energy and Mass Model of Snow Cover Suitable for Operational Avalanche Forecasting, *Journal of Glaciology*, 35, 333–342, <https://doi.org/10.3189/s0022143000009254>, 1989.
- Brun, E., David, P., Sudul, M., and Brunot, G.: A numerical model to simulate snow-cover stratigraphy for operational avalanche forecasting, 760 *Journal of Glaciology*, 38, 13–22, <https://doi.org/10.1017/s0022143000009552>, 1992.
- Calonne, N., Flin, F., Morin, S., Lesaffre, B., du Roscoat, S. R., and Geindreau, C.: Numerical and experimental investigations of the effective thermal conductivity of snow, *Geophysical Research Letters*, 38, L23 501, <https://doi.org/10.1029/2011GL049234>, 2011.
- Calonne, N., Geindreau, C., and Flin, F.: Macroscopic Modeling for Heat and Water Vapor Transfer in Dry Snow by Homogenization, *The Journal of Physical Chemistry B*, 118, 13 393–13 403, <https://doi.org/10.1021/jp5052535>, 2014.
- 765 Domine, F., Barrere, M., and Sarrazin, D.: Seasonal evolution of the effective thermal conductivity of the snow and the soil in high Arctic herb tundra at Bylot Island, Canada, *The Cryosphere*, 10, 2573–2588, <https://doi.org/10.5194/tc-10-2573-2016>, 2016.
- Domine, F., Picard, G., Morin, S., Barrere, M., Madore, J.-B., and Langlois, A.: Major Issues in Simulating Some Arctic Snowpack Properties Using Current Detailed Snow Physics Models: Consequences for the Thermal Regime and Water Budget of Permafrost, *Journal of Advances in Modeling Earth Systems*, 11, 34–44, <https://doi.org/10.1029/2018ms001445>, 2019.
- 770 Farlow, S. J.: *Partial Differential Equations for Scientists and Engineers*, Dover Publications, Mineola, New York, USA, reprint of the John Wiley & Sons, New York, USA, 1982 edition, 1993.
- Hansen, A. and Foslien, W.: A macroscale mixture theory analysis of deposition and sublimation rates during heat and mass transfer in dry snow, *The Cryosphere*, 9, 1857–1878, <https://doi.org/10.5194/tc-9-1857-2015>, 2015.
- Huang, K., Zhang, R., and van Genuchten, M. T.: An Eulerian-Lagrangian approach with an adaptively corrected method of characteristics 775 to simulate variably saturated water flow, *Water Resources Research*, 30, 499–507, <https://doi.org/10.1029/93WR02881>, 1994.
- Jafari, M., Gouttevin, I., Couttet, M., Wever, N., Michel, A., Sharma, V., Rossmann, L., Maass, N., Nicolaus, M., and Lehning, M.: The Impact of Diffusive Water Vapor Transport on Snow Profiles in Deep and Shallow Snow Covers and on Sea Ice, *Frontiers in Earth Science*, 8, 249, <https://doi.org/10.3389/feart.2020.00249>, 2020.
- Johnson, J. B.: Snow Deformation, in: *Encyclopedia of Earth Sciences Series*, pp. 1041–1045, Springer, Dordrecht, Netherlands, 780 https://doi.org/10.1007/978-90-481-2642-2_501, 2011.
- Kirchner, H. K., Michot, G., Narita, H., and Suzuki, T.: Snow as a foam of ice: Plasticity, fracture and the brittle-to-ductile transition, *Philosophical Magazine A*, 81, 2161–2181, <https://doi.org/10.1080/01418610108217141>, 2001.
- Kowalski, J. and Torrilhon, M.: Moment Approximations and Model Cascades for Shallow Flow, *Communications in Computational Physics*, 25, 669–702, <https://doi.org/10.4208/cicp.oa-2017-0263>, 2019.
- 785 Krinner, G., Derksen, C., Essery, R., Flanner, M., Hagemann, S., Clark, M., Hall, A., Rott, H., Brutel-Vuilmet, C., Kim, H., Ménard, C. B., Mudryk, L., Thackeray, C., Wang, L., Arduini, G., Balsamo, G., Bartlett, P., Boike, J., Boone, A., Chéruy, F., Colin, J., Cuntz, M., Dai,

- Y., Decharme, B., Derry, J., Ducharne, A., Dutra, E., Fang, X., Fierz, C., Ghattas, J., Gusev, Y., Haverd, V., Kontu, A., Lafaysse, M., Law, R., Lawrence, D., Li, W., Marke, T., Marks, D., Ménégos, M., Nasonova, O., Nitta, T., Niwano, M., Pomeroy, J., Raleigh, M. S., Schaedler, G., Semenov, V., Smirnova, T. G., Stacke, T., Strasser, U., Svenson, S., Turkov, D., Wang, T., Wever, N., Yuan, H., Zhou, W., and Zhu, D.: ESM-SnowMIP: assessing snow models and quantifying snow-related climate feedbacks, *Geoscientific Model Development*, 11, 5027–5049, <https://doi.org/10.5194/gmd-11-5027-2018>, 2018.
- 790 Lacroix, M. and Garon, A.: Numerical Solution of phase change problems: an Eulerian-Lagrangian approach, *Numerical Heat Transfer, Part B*, 19, 57–78, <https://doi.org/10.1080/10407799208944922>, 1992.
- Lehning, M., Bartelt, P., Brown, B., Fierz, C., and Satyawali, P.: A physical SNOWPACK model for the Swiss avalanche warning: Part II. Snow microstructure, *Cold Regions Science and Technology*, 35, 147–167, [https://doi.org/10.1016/s0165-232x\(02\)00073-3](https://doi.org/10.1016/s0165-232x(02)00073-3), 2002.
- 795 LeVeque, R. J.: *Finite Volume Methods for Hyperbolic Problems*, Cambridge Texts in Applied Mathematics, Cambridge University Press, <https://doi.org/10.1017/CBO9780511791253>, 2002.
- Libbrecht, K. G.: Physical properties of ice, <http://www.cco.caltech.edu/~atomic/snowcrystals/ice/ice.htm>, last access: 29 July 2021, 1999.
- Lundin, J. M., Stevens, C. M., Arthern, R., Buizert, C., Orsi, A., Ligtenberg, S. R., Simonsen, S. B., Cummings, E., Essery, R., Leahy, W., Harris, P., Helsen, M. M., and Waddington, E. D.: Firn Model Intercomparison Experiment (FirnMICE), *Journal of Glaciology*, 63, 401–422, <https://doi.org/10.1017/jog.2016.114>, 2017.
- 800 Mellor, G. L. and Blumberg, A. F.: Modeling Vertical and Horizontal Diffusivities with the Sigma Coordinate System, *Monthly Weather Review*, 113, 1379–1383, [https://doi.org/10.1175/1520-0493\(1985\)113<1379:mvaHDw>2.0.co;2](https://doi.org/10.1175/1520-0493(1985)113<1379:mvaHDw>2.0.co;2), 1985.
- Meyer, C. R., Keegan, K. M., Baker, I., and Hawley, R. L.: A model for French-press experiments of dry snow compaction, *The Cryosphere*, 14, 1449–1458, <https://doi.org/10.5194/tc-14-1449-2020>, 2020.
- 805 Morland, L., Kelly, R., and Morris, E.: A mixture theory for a phase-changing snowpack, *Cold Regions Science and Technology*, 17, 271–285, [https://doi.org/10.1016/s0165-232x\(05\)80006-0](https://doi.org/10.1016/s0165-232x(05)80006-0), 1990.
- Morland, L. W.: A fixed domain method for diffusion with a moving boundary, *Journal of Engineering Mathematics*, 16, 259–269, <https://doi.org/10.1007/bf00042720>, 1982.
- 810 Paterson, W.: *The Physics of Glaciers*, Pergamon international library of science, technology, engineering and social studies, Elsevier, 1994.
- Schweizer, J., Jamieson, J. B., and Schneebeli, M.: Snow avalanche formation, *Reviews of Geophysics*, 41, 1016, <https://doi.org/10.1029/2002rg000123>, 2003.
- Schürholt, K., Kowalski, J., and Löwe, H.: Elements of future snowpack modeling - part 1: A physical instability arising from the non-linear coupling of transport and phase changes, *The Cryosphere*, <https://doi.org/doi.org/10.5194/tc-2021-72>, preprint of Part 1 of the companion paper, 20202021.
- 815 Viallon-Galinier, L., Hagenmuller, P., and Lafaysse, M.: Forcing and evaluating detailed snow cover models with stratigraphy observations, *Cold Regions Science and Technology*, 180, 103–163, <https://doi.org/10.1016/j.coldregions.2020.103163>, 2020.
- Vionnet, V., Brun, E., Morin, S., Boone, A., Faroux, S., Moigne, P. L., Martin, E., and Willemet, J.-M.: The detailed snowpack scheme Crocus and its implementation in SURFEX v7.2, *Geoscientific Model Development*, 5, 773–791, <https://doi.org/10.5194/gmd-5-773-2012>, 2012.
- 820 Wever, N., Fierz, C., Mitterer, C., Hirashima, H., and Lehning, M.: Solving Richards Equation for snow improves snowpack meltwater runoff estimations in detailed multi-layer snowpack model, *The Cryosphere*, 8, 257–274, <https://doi.org/10.5194/tc-8-257-2014>, 2014.
- Wever, N., Valero, C. V., and Fierz, C.: Assessing wet snow avalanche activity using detailed physics based snowpack simulations, *Geophysical Research Letters*, 43, 5732–5740, <https://doi.org/10.1002/2016GL068428>, 2016.

Wiese, M. and Schneebeil, M.: Early-stage interaction between settlement and temperature-gradient metamorphism, *Journal of Glaciology*, 825 63, 652–662, <https://doi.org/10.1017/jog.2017.31>, 2017.

Wingham, D. J.: Small fluctuations in the density and thickness of a dry firn column, *Journal of Glaciology*, 46, 399–411, <https://doi.org/10.3189/172756500781833089>, 2000.